Metrics for ~~assessing Linear Inverse Problems~~evaluating the "quality" in linear atmospheric inverse problems: a case study of a ~~Trace Gas Inversion~~trace gas inversion

Vineet Yadav[1], Subhomoy Ghosh[2,3], and Charles E. Miller[1]

[1]Jet Propulsion Laboratory, California Institute of Technology, 4800 Oak Grove Drive, Pasadena, CA, USA
[2]University of Notre Dame, Notre Dame, IN, USA
[3]National Institute of Standards and Technology, Gaithersburg, MD, USA

Correspondence: Subhomoy Ghosh (sghosh4@nd.edu)

Abstract. ~~Multiple~~ Several metrics have been proposed and utilized to ~~assess~~ diagnose the performance of linear Bayesian and geostatistical atmospheric inverse problems. These metrics are mostly related to assessing reduction in prior uncertainties, comparing modeled observations to true observations, and checking distributional assumptions. These metrics~~though important~~, though important, should be augmented with sensitivity analysis to obtain a comprehensive understanding of the performance of atmospheric inversions and critically improve the quality of an atmospheric inverse model and confidence in the estimated fluxes. ~~With this motivation~~In this study, we derive analytical forms of the local sensitivities of the estimated fluxes with respect to the number of inputs such as measurements, covariance parameters, covariates, and forward operator~~or jacobian.~~. These local sensitivities have different units and vastly different magnitudes. To this end, we also propose a technique to rank local sensitivities. In addition to local sensitivity, we ~~develop~~ provide a framework for global sensitivity analysis for linear atmospheric inversion that shows the apportionment of the uncertainty ~~of~~ in different inputs to ~~an inverse problem. The proposed framework is applicable to any other domain that employs linear Bayesian and geostatistical inverse methods.~~ the uncertainty of estimated fluxes. Prior to performing an inversion, we also propose a mathematical framework to construct correlation matrices from a pre-computed forward operator that encompasses non-stationary structures. This is closely tied to the overall quality of estimated fluxes. We show the application of our methodology in the context of an atmospheric inverse problem for estimating ~~urban GHG emissions~~ methane fluxes in Los Angeles~~. Within its context, we also propose a mathematical framework to construct correlation functions and components of uncertainty matrices from a pre-computed jacobian that encompasses non-stationary structures~~, California. The proposed framework is applicable to any other domain that employs linear Bayesian and geostatistical inverse methods.

1 Introduction

Inverse models within the context of atmospheric applications are often used for constraining global to regional scale fluxes of trace gases (for discussion see, Enting, 2002). At global scale, data assimilation (for further details on data assimilation, see Wikle and Berliner, 2007) that sequentially assimilates observations and updates the prior estimates of fluxes by utilizing an

atmospheric model coupled with chemistry remains the primary inverse modeling framework. This framework at regional scale is complimented by inversions that assimilates all observations simultaneously by utilizing a ~~pre-computed forward operator or jacobian~~ precomputed forward operator (Lin et al., 2003) that describes the relationship between observations and fluxes (for details, see Enting, 2002). This work focuses on these latter class of inverse methods. It specifically addresses sensitivity analysis and correlation in the ~~jacobian~~ forward operator in the context of Bayesian (for e.g., see Lauvaux et al., 2016) and geostatistical inverse methods (see Kitanidis, 1996).

The senstivity analysis in context of this study is covered under local and global themes. Primarily, we focus on local sensitivity analysis (LSA) that ~~computes measure of~~ measures the effect of a given input on a given output. This is obtained by computing partial derivatives of an output of interest with respect to an input factor (See Rabitz, 1989, and Turányi, 1990). Within global theme, we focus on how uncertainty in the model output can be apportioned to different sources of uncertainty with respect to corresponding model input (Saltelli et al., 2008).

Previously, many methods have been proposed and utilized to perform sensitivity analysis. These can be categorized as global and local sensitivity analyses. Global sensitivity analysis (GSA) includes Morris's (e.g. Morris, 1991) one step at a time method (OAT), Polynomial Chaos Expansion (PCE) (e.g. Sudret, 2008), Fourier amplitude sensitivity test (FAST) (e.g. Xu and Gertner, 2011), Sobol's method (e.g. Sobol, 2001) and Derivative based global sensitivity measures (DGSM) (e.g. Sobol and Kucherenko, 2010) among others. These existing GSA methods either: (1) assume independence of parameters (e.g., FAST and OAT), or are (2) computationally expensive (e.g., Sobol's method), or (3) require knowledge of the joint probability distribution of the parameter space (e.g., DGSM, PCE). Therefore, these traditional methods cannot be directly applied in linear atmospheric inverse problems, which consists of tens of thousands of non-normal, spatio-temporally correlated parameters (includes observations). Recently proposed active subspace based GSA (Constantine and Diaz, 2017) uses low dimensional approximation of the parameter space. In its current form, it is still computationally expensive for problems that consists of thousands of parameters (see case study in Constantine and Diaz, 2017).

In comparison to GSA, local sensitivity method like Bayesian Hyper Differential Sensitivity Analysis (HDSA) computes partial derivatives with respect to maximum a posteriori probability estimates (MAP) of a quantity of interest. Our method for LSA is similar to Bayesian HDSA, except for the fact that it directly finds analytical derivatives of the MAP solution with respect to the input parameters in linear atmospheric inverse problems. This is possible when we know analytical closed form solutions of the estimated fluxes. In this study, we leverage a framework that is not only one of the most commonly adopted forms in atmospheric inversions but also admit closed form solutions. Thus, unlike the previous work on Bayesian HDSA, we do not generate samples from the prior to compute multiple MAP points. As we have limited knowledge of the prior distribution of the spatio-temporally correlated parameters. We derive exact functional form of the local sensitivity equations based on the closed form analytical MAP solution. Our method is simple and amenable to tens of thousands of parameters. Note as in all linear atmospheric inverse problems one of the key goals of this work is to study the importance of thousands of

spatio-temporally varying parameters by ranking them and computation of the local sensitivities is a means to achieve that goal.

Overall, in atmospheric trace gas inversions mostly LSA is performed. Within this context, LSA asseses how sensitive the posterior estimates of fluxes are with reference to the underlying choices or assumptions, like (1) observations included, (2) model-data error covariance, (3) the input prior information and its error, and (4) the ~~jacobian~~ forward operator (for discussion see, Michalak et al., 2017). This task is sometimes performed to arrive at a robust estimate of fluxes and their uncertainties. It is achieved by running an inverse model multiple times by varying the inputs and assessing their impact on the estimated fluxes and uncertainties. Another complimentary way to do LSA is by computing local partial derivatives with respect to these quantities down to an individual entry that go in an inversion.

LSA can be grouped with standard information content approaches such as averaging kernel or model resolution matrix and degrees of freedom for signal (DOFS; for details see ~~section~~Sec. 3.2.1 of this manuscript, Rodgers, 2000, and Brasseur and Jacob, 2017). Averaging kernel matrix shows how the estimated fluxes are related or sensitive to the true fluxes. Thus, it belongs to the LSA category. However, LSA is more informative than DOFS and averaging kernel alone as it goes after individual components (see ~~section~~Sec. 3.2) that determine DOFS. Furthermore, DOFS is a measure that provides an estimate of the information resolved by an inversion. In comparison, LSA focuses on quantifying the impact and the relative importance of various components of an inversion in governing the estimates of fluxes.

In this ~~work, we provide~~ study, we focus on the quality of the inverse estimates of the fluxes which means providing diagnostic metrics to better characterize our understanding of the impact of input choices on the inverse estimates of fluxes and thus improve the quality of the inverse model. Specifically, in this technical note we provide: (1) analytical expressions to conduct post hoc (that is after an inversion has been performed) LSA ~~through local partial derivatives. In order to provide a complete framework ,~~ by computing partial derivatives, (2) a scientifically interpretable framework for ranking thousands of spatio-temporally correlated input parameters with same or different units, (3) a mathematical schema for ~~global sensitivity analysis (GSA) is also discussed but it remains considerably harder~~ conducting GSA. However, GSA is considerably difficult to perform in the absence of the knowledge about the uncertainties associated with all the inputs that go in an inversion~~.~~

~~We also develop methods~~ , and (4) a technique to assess spatio-temporal correlation between ~~jacobians~~ forward operators of two or multiple observations. This is tied to the overall diagnostics of the estimated fluxes as fluxes ~~remain highly~~ are strongly sensitive to the ~~jacobian~~ forward operator and improvement in understanding the representation of ~~atmospheric transport~~ the atmospheric transport model error through spatio-temporal association in the ~~jacobian~~ forward operators can lead to significant improvement in designing the components of ~~a suitable~~ an atmospheric inversion framework.

2 Organization of the study

We have divided this workin to two parts. In the first part (Section ??) In a generic form a linear inverse problem can be written as:

$$\mathbf{z} = \mathbf{H}\mathbf{s} + \epsilon \tag{1}$$

where $\mathbf{H}$ is a forward operator that maps model parameters $\mathbf{s}$ (fluxes in the context of this work) to measurements $\mathbf{z}$ and encapsulates our understanding of the physics of the measurements. The error ϵ in Eq. (1) describes the mismatch between measurements and the modeled measurements (see Sec. 3).

In a typical linear atmospheric inverse problem (see Fig. 1) the estimates of the fluxes (box 8 of Fig. 1) are obtained in a classical one stage batch Bayesian setup (for details see Enting, 2002; Tarantola, 2005), where the a priori term (box 3 in Fig. 1) is based on a fixed flux pattern at a prescribed spatio-temporal resolution, and errors (box 6 in Fig. 1) are either assumed to be independent or are governed by a prescribed covariance structure (for details see Gurney et al., 2003; Rödenbeck et al., 2003, 2006).

Within the previously mentioned setup, choice of the input parameters including the forms of error structures have profound impact on the quality of the inverse estimates of fluxes. Understanding the impact of these inputs is critical for evaluating the quality of estimated fluxes. Thus, in the first part of this work we utilize the understanding of the physics of the measurement that is encapsulated in $\mathbf{H}$ to generate correlation matrices that are scientifically interpretable in the context of estimated fluxes and to build an interpretable non-stationary model of the residual covariance structure (box 6 in Fig. 1). This is described in Sec. 3.1. In the second part of this work we assess and rank the importance of the inputs mentioned in the middle column (the green background box) of Fig. 1 in governing the estimates of fluxes (box 8 of Fig. 1). This is covered in Sec. 3.2. These two parts are followed by a methane (CH_4) case study that demonstrates the applicability of our methods (i.e., Sectionsee Sec. 4).

To maintain maximum transparency, facilitate assessment, and show applicability of our methods in SectionSec. 3 we also provide two well documented interactive MATLAB Live scripts Livescripts (for details on Live script Livescript see MatlabLivescript), one for each methodological partthat contains . These Livescripts contain equations, code, and visualizations as it relates to the real-data case study described in Section 4. All of these Sec. 4, and are included as supplementary material. Separate pdfs of these Live scripts Livescripts are also included for the readers who do not have access to MATLAB.

3 Methods and derivation

3.1 Analysis of the jacobianforward operator

In inversions that assimilates all observations simultaneously, first a jacobian forward operator for each observation that would be included in an inversion is obtained from a transport model. These observations of trace gases can be obtained from multiple platforms that include in-situ network of fixed locations on the surface, intermittent aircraft flights and satellites. In most situa-

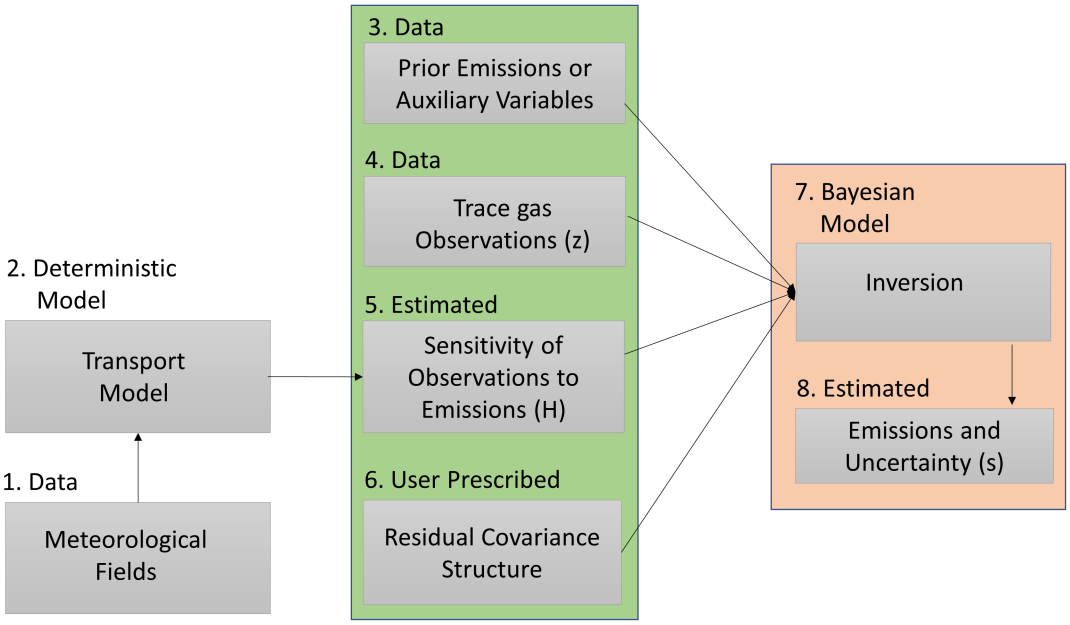

Figure 1. The schema for performing a linear atmospheric inversion to obtain estimates of the fluxes of greenhouse gases. The middle column (the green background box) lists all the inputs that are required for performing an inversion whereas the right column (the orange background box) lists the modeling process (box 7) and the output obtained after performing an inversion (box 8). Note this work focuses on understanding and ranking the impact of the inputs (box 3, ~~we provide diagnostics associated with the jacobian.This is done as these derivations can be deployed for assessment of the jacobian prior to or separately from an inversion . In the second part (Section 3.2), we cover local and global sensitivity analysis that can only be conducted after inverse estimation of the fluxes.~~ 4, and 6 in the middle column) on the estimates of fluxes (box 8) and developing correlation structures from the forward operator (box 5).

tions, the spatio-temporal ~~coverages of these jacobians~~ coverage of these forward operators are visually assessed by plotting an aggregated sum or mean of their values over a map of the spatial domain of the study. However, standard quantitative metrics to assess their coverage and intensity in space and time remains completely absent. In this study, we present two metrics for this assessment and these are defined below. These metrics conform to triangular inequality and therefore can be defined as distance function in their respective metric spaces.

Note sometimes in the published literature on trace gas inversions the ~~jacobian~~ forward operator obtained from a transport model is referred to as a sensitivity matrix, Jacobian or footprint. Henceforth, to avoid misinterpretation, we always refer to ~~jacobian as footprint~~ Jacobian/sensitivity matrix/footprint as forward operator. We show our application through ~~footprints~~

forward operators constructed by running a Lagrangian transport model. However, our methods can also be applied in analytical Eulerian framework (see Brasseur and Jacob, 2017 for details).

3.1.1 Integrated area overlap measurement index (IAOMI)

The Integrated Area Overlap Measurement Index (IAOMI) summarizes the shared information content between two ~~footprints~~ forward operators and hence indirectly between two observations~~under the assumption that error in dispersion and transport is absent and the sources of emissions are uniformly distributed.~~ . It is therefore a measure of the uniqueness of the flux signal associated with an observation in comparison to other observations.

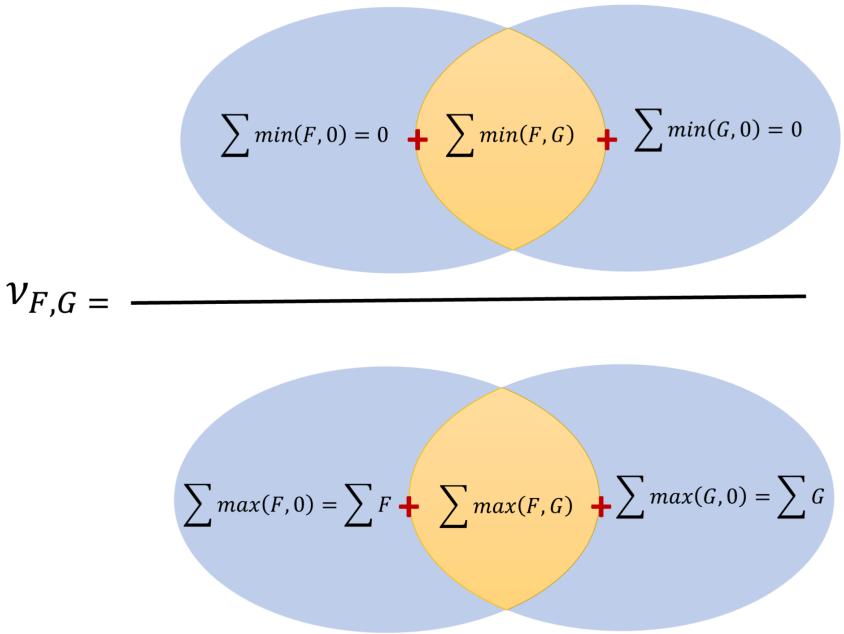

Figure 2. Venn diagram that defines IOAMI in terms of two hypothetical ~~footprints F and G~~forward operators $\mathbf{F}$ and $\mathbf{G}$

Intuitively, IAOMI can be ~~understood in terms of functions on sets. For e.g., given two footprints we can consider their entries or intensities as two sets indexed by spatio-temporal coordinates. Within such a context of sets, IOAMI is just~~ better understood spatially. For a given time point, consider two forward operators $\mathbf{F}$ and $\mathbf{G}$ as two vector-valued functions over an area. IOAMI is the proportion of the common contribution of the two ~~footprints~~ forward operators from the intersected area with respect to the overall contribution of the two ~~footprints~~forward operators. This is demonstrated through a Venn diagram in ~~Figure~~Fig. 2. Thus, IAOMI can be defined as:

$$\nu_{F,G} = \frac{\Sigma_{A_F \cap A_G} H_1(F,G)}{\Sigma_{A_F \cup A_G} H_2(F,G)} \nu_{\mathbf{F},\mathbf{G}} = \frac{\Sigma_{A_\mathbf{F} \cap A_\mathbf{G}} \mathbf{f}_1(\mathbf{F},\mathbf{G})}{\Sigma_{A_\mathbf{F} \cup A_\mathbf{F}} \mathbf{f}_2(\mathbf{F},\mathbf{G})} \quad (2)$$

Where for any ~~footprint S~~forward operator $\mathbf{S}$, the corresponding set ~~A_S on which footprints are~~ $A_{\mathbf{S}}$ on which forward operator is always positive, is defined as ~~$A_S = \{(i,j,t) : (i,j) \in \mathcal{D}, t \in T, S(i,j,t) > 0\}$. The functionals H_1 and H_2 are functions of the two footprints under comparison and are defined~~ $A_{\mathbf{S}} = \{\boldsymbol{x} : \mathbf{S}(\boldsymbol{x}) > 0\}$ and the two vector-valued functionals $\mathbf{f}_1$ and $\mathbf{f}_2$ can be given as:

$$\mathbf{f}_1(\mathbf{F},\mathbf{G}) = \begin{cases} min(\mathbf{F},\mathbf{G}) & \text{on } A_{\mathbf{F}} \cap A_{\mathbf{G}} \\ 0 & \text{otherwise} \end{cases} \quad \text{and} \quad \mathbf{f}_2(\mathbf{F},\mathbf{G}) = \begin{cases} max(\mathbf{F},\mathbf{G}) & \text{on } A_{\mathbf{F}} \cap A_{\mathbf{G}} \\ \mathbf{F} & \text{on } A_{\mathbf{F}} \cap A_{\mathbf{G}}^c \\ \mathbf{G} & \text{on } A_{\mathbf{F}}^c \cap A_{\mathbf{G}} \end{cases} \tag{3}$$

Note that ~~, the $\nu_{F,G}$ defined above~~ the IAOMI defined in Eq. (2) can also be written as a ~~simple~~ ratio of the sum ~~over~~ of minimums over sum of the maximums ~~.~~as:

$$\nu_{F,G\mathbf{F},\mathbf{G}} = \frac{\Sigma_{A_F \cup A_G} min(F,G)}{\Sigma_{A_F \cup A_G} max(F,G)} \frac{\Sigma_{A_{\mathbf{F}} \cup A_{\mathbf{G}}} min(\mathbf{F},\mathbf{G})}{\Sigma_{A_{\mathbf{F}} \cup A_{\mathbf{G}}} max(\mathbf{F},\mathbf{G})} \tag{4}$$

~~Thus,~~ IAOMI ν can also be thought as a measure of similarity between two ~~footprints~~forward operators. It is evident from ~~equation 4~~ Eq. (4) that this is a weighted Jaccard similarity index or Ruzicka index (Cha, 2007). It follows that ν is closed and bounded in $[0,1]$ and accounts for both the spatio-temporal spread and the intensity of the ~~footprint~~forward operator. A stronger ν implies larger overlap of intensity in space and time and is analogous to finding the common area within two curves. The corresponding measure of dissimilarity can be defined by $1-\nu$. The smaller the overlap or the larger the value of $1-\nu$, the larger is the dissimilarity. Note the ν metric is only indicative of the overlap in the spatio-temporal intensity between two ~~footprints~~forward operators. To measure how much of the shared intensity has come from either ~~footprint~~forward operator, we use a metric ~~$I_{\nu_F} \upsilon_{\mathbf{F}|(\mathbf{F},\mathbf{G})}$~~ defined as:

$$I_{\nu_F} \upsilon_{\mathbf{F}|(\mathbf{F},\mathbf{G})} = \frac{\Sigma_{A_F \cap A_G} H_1(F,G)}{\Sigma_{A_F} H_3(F)} \frac{\Sigma_{A_{\mathbf{F}} \cap A_{\mathbf{G}}} \mathbf{f}_1(\mathbf{F},\mathbf{G})}{\Sigma_{A_{\mathbf{F}}} \mathbf{f}_3(\mathbf{F})} \tag{5}$$

Where ~~$H_3(F) = F$ on A_F~~ $\mathbf{f}_3(\mathbf{F}) = F$ on $A_{\mathbf{F}}$ and 0 everywhere else. Likewise, we can define ~~$I_{\nu_G} \upsilon_{\mathbf{G}|(\mathbf{F},\mathbf{G})}$~~ which shows proportional contribution of the ~~footprint~~ forward operator G on the shared intensity. Both ν and ~~$I_\nu \upsilon$~~ can be computed from observations taken from same or different platforms, at same or different time or for two different in-situ measurement sites over a specified time-interval.

3.1.2 Spatio-temporal Area of Dominance (STAD)

The notion of the spatio-temporal area of dominance (STAD) stems naturally from IAOMI. For any two ~~footprints F, and G~~forward operators $\mathbf{F}$, and $\mathbf{G}$, we can find out the left-over dominant contribution of ~~F and G~~ $\mathbf{F}$ and $\mathbf{G}$ by computing quantities ~~$F - G$ and $G - F$~~ $\mathbf{F} - \mathbf{G}$ and $\mathbf{G} - \mathbf{F}$ that leads to determination of the area where ~~F or G~~ $\mathbf{F}$ or $\mathbf{G}$ is dominant.

~~Mathematically, for two footprints F and G~~For two forward operators $\mathbf{F}$ and $\mathbf{G}$, STAD of ~~F~~ $\mathbf{F}$ with respect to ~~G~~ $\mathbf{G}$ is defined as:

$$\text{STAD}_{F\,\mathbf{F}}(F,G) = \begin{cases} \mathbf{F} - min(\mathbf{F},\mathbf{G}) & \text{on } A_{\mathbf{F}} \cap A_{\mathbf{G}} \\ \mathbf{F} & \text{otherwise} \end{cases}$$

IAOMI and STAD of any ~~footprint F~~ forward operator $\mathbf{F}$ with respect to the ~~footprints F and G~~ forward operators $\mathbf{F}$ and $\mathbf{G}$ are linked by the following equation:

$$\nu_{F,G\,\mathbf{F},\mathbf{G}} \Sigma_{A_{\mathbf{F}} \cup A_{\mathbf{G}}}\, H_2(F,G) + \Sigma \text{STAD}_{F\,A_{\mathbf{F}} \cup A_{\mathbf{G}}}\, STAD_{\mathbf{F}}(F,G) = \Sigma_{A_{\mathbf{F}}} F \text{ on } A_F \cup A_G \tag{6}$$

Given a ~~set of footprints $\{F, G_1, \cdots, G_K\}$~~number of forward operators $\{\mathbf{F}, \mathbf{G}_1, \mathbf{G}_2, \cdots\}$, STAD for any particular ~~footprint F~~ forward operator $\mathbf{F}$ with respect to all other ~~footprints~~ forward operators can be generalized from ~~equation 6 as $F_{\text{STAD}}(F, H_{-F})$ where $H_{-F} = \max_k G_k$ on A_G; $A_G = \cup_k A_{G_k}$. A_{G_k}~~ Eq. (6) as $\mathbf{F}_{\text{STAD}}(\mathbf{F}, \mathbf{G}_{\max})$ where $\mathbf{G}_{\max} = \max_i \mathbf{G}_i$ on $A_{\mathbf{G}}$; $A_{\mathbf{G}} = \cup_k A_{\mathbf{G}_k}$ and $A_{\mathbf{G}_k}$ is the set on which ~~footprint G_k~~ forward operator $\mathbf{G}_k$ is always positive (see ~~section~~Sec. 3.1.1 for ~~it's~~ its definition). STAD can be aggregated over any time-periods. Intuitively, STAD determines areas in space-time where one ~~footprint~~ forward operator dominates over other ~~footprints~~forward operators. This is especially useful in locating the primary sources of ~~emissions~~ fluxes that influences an observation.

3.1.3 Jensen-Shannon distance (JSD) for ~~footprints~~forward operators

Dissimilarity between ~~footprints~~ forward operators can also be measured via entropy (for definition, see MacKay et al., 2003) based distances. Entropy distances are sensitive in capturing differences between two distributions that are similar in ~~1st~~ the first order (e.g. mean, or median) and second order moments (e.g. variance, or quartile deviation) but differ in higher order moments (e.g. Kurtosis) or modes (e.g. unimodal vs. multimodal). Entropy based distance metrics that adhere to triangular inequality can also be combined with spatio-temporal coverage to measure the probabilistic divergence between two ~~footprints~~forward operators. One such metric is Jensen-Shanon distance (JSD) (Nielsen, 2019) which can be used to compute distance between two distributions generated by the ~~footprints. Normalized footprints~~ forward operators. Normalized forward operators can be seen as samples from an underlying high-dimensional probability distribution such that total sum is one. For any ~~particular time point t, this~~ vector-valued forward operator $\mathbf{F}$, normalization by the total sum ~~, for a vectorized footprint ($F(i,j,t)$ can be written as $F(k,t)$ where k spans over all combinations of i and j) of an observation can be~~ can be given as:

$$P_{F(k,t)\,F_k} = \frac{F(k,t)}{\sum_{k=1}^{g} F(k,t)} \frac{F_k}{\sum_k F_k} \tag{7}$$

where ~~P denotes a probability measure.~~ F_k denotes k^{th} entry of $\mathbf{F}$ and index k spans over the entire domain. The symbol P denotes normalized forward operator. We can then use JSD to compute distance between two ~~footprint induced probability distributions. After normalization~~normalized forward operators. Thus, JSD can be computed as:

$$JSD\left(P_{F\mathbf{F}}||P_{G\mathbf{G}}\right) = \sqrt{\frac{1}{2}D\left(P_{F\mathbf{F}}||M\right) + \frac{1}{2}D\left(P_{G\mathbf{G}}||M\right)} \tag{8}$$

where D stands for Kulback-Leibler (KL) divergence (see MacKay et al., 2003 for details). KL divergence D of any probability ~~measure~~ distribution p with respect to another probability ~~measure~~ distribution q is defined as: $D(p||q) = \sum p\log(p/q)$ ~~.~~ and M is defined as: ~~$M = \frac{1}{2}(P_F + P_G)$~~ $M = \frac{1}{2}(P_{\mathbf{F}} + P_{\mathbf{G}})$. The symbol $||$ is used to indicate that ~~$D(P_F||M)$ and $D(P_G||M)$~~ $D(P_{\mathbf{F}}||M)$ and $D(P_{\mathbf{G}}||M)$ are not conditional entropies (see MacKay et al., 2003). JSD is closed and bounded in $[0, 1]$ when KL divergence is computed with base 2 logarithm. Intuitively, JSD and $1-\nu$ (i.e. 1-IAOMI) are comparable since both of them are measures of dissimilarity.

Note that, one can use JSD or 1-IAOMI matrix of all pairwise ~~footprints~~ forward operators as a representative distance matrix for describing correlations in model-data errors (i.e., $\mathbf{R}$ in ~~equation 9). This~~ Eq. (9)). These correlation matrices need to be at least positive semi-definite. Since JSD or 1-IAOMI matrices are real, symmetric, and admit orthogonal decomposition, ~~element-wise~~ entry-wise exponential of such symmetric diagonalizable matrices ~~would be~~ is positive-semidefinite. Thus, they can be incorporated in $\mathbf{R}$ via the commonly adopted exponential kernel of the distance matrix (see Ghosh et al., 2021). Furthermore, the IAOMI matrix itself is a positive semidefinite (Bouchard et al., 2013) matrix and can also be directly incorporated in ~~R~~ $\mathbf{R}$ as a measure of correlation. However, we do not explore this area of research in this manuscript.

3.2 Local sensitivity analysis in inversions

For linear Bayesian and geostatistical inverse problem, the solutions (see, Tarantola, 2005 for the batch Bayesian and Kitanidis, 1996 for the geostatistical case) can be obtained by minimizing their respective objective functions. These objective functions can be given ~~by equations 9 and 10~~ as:

$$L(\mathbf{s}\mathbf{s}|\mathbf{y}\mathbf{y}, \mathbf{s}_{\text{prior}}\mathbf{s}_{\text{prior}}, \mathbf{H}\mathbf{H}, \mathbf{Q}\mathbf{Q}, \mathbf{R}\mathbf{R}) = \frac{1}{2}(\mathbf{z}\mathbf{z} - \mathbf{H}\mathbf{s}\mathbf{H}\mathbf{s})^T\mathbf{R}^t\mathbf{R}^{-1}(\mathbf{z}\mathbf{z} - \mathbf{H}\mathbf{s}\mathbf{H}\mathbf{s}) + \frac{1}{2}(\mathbf{s}\mathbf{s} - \mathbf{s}_{\text{prior}}\mathbf{s}_{\text{prior}})^T\mathbf{Q}^t\mathbf{Q}^{-1}(\mathbf{s}\mathbf{s} - \mathbf{s}_{\text{prior}}\mathbf{s}_{\text{prior}}) \tag{9}$$

$$L(\mathbf{s}\mathbf{s}|\mathbf{y}\mathbf{y}, \mathbf{H}\mathbf{H}, \mathbf{Q}\mathbf{Q}, \mathbf{R}\mathbf{R}, \boldsymbol{\beta}) = \frac{1}{2}(\mathbf{z}\mathbf{z} - \mathbf{H}\mathbf{s}\mathbf{H}\mathbf{s})^T\mathbf{R}^t\mathbf{R}^{-1}(\mathbf{z}\mathbf{z} - \mathbf{H}\mathbf{s}\mathbf{H}\mathbf{s}) + \frac{1}{2}(\mathbf{s}\mathbf{s} - \mathbf{X}\boldsymbol{\beta}\mathbf{X}\boldsymbol{\beta})^T\mathbf{Q}^t\mathbf{Q}^{-1}(\mathbf{s}\mathbf{s} - \mathbf{X}\boldsymbol{\beta}\mathbf{X}\boldsymbol{\beta}) \tag{10}$$

where lower case symbols represent vectors ~~,~~ and the uppercase symbols represent matrices, and this same approach of representation is adopted throughout the manuscript. In ~~equation 9 and 10, $\mathbf{z}_{(n,1)}$ with units ppm are available measurements . $\mathbf{H}_{(n,m)}$ with units~~ Eq. (9) and (10), $\mathbf{z}$ is an $(n \times 1)$ vector of available measurements with unit of each entry being ppm. The forward operator $\mathbf{H}$ is an $(n \times m)$ matrix with unit of each entry being ppm μmoles^{-1}m^{2}sec~~is a footprint, .~~ The matrix $\mathbf{H}$ is obtained from a transport model that describes the relationship between measurements and unknown fluxes. ~~$\mathbf{s}_{(m,1)}$ are unknown fluxes that have units~~ Unknown flux $\mathbf{s}$ is an $(m \times 1)$ vector with unit of entries being μmoles m^{-2}sec^{-1}. ~~$\mathbf{R}_{(n,n)}$ with~~

units ppm^2 is the covariance The covariance matrix $\mathbf{R}$ of the model-data errors . $\mathbf{X}_{(m,p)}$ are is an $(n \times n)$ matrix with unit of the entries being ppm^2. The covariate matrix $\mathbf{X}$ is an $(m \times p)$ matrix of known covariates related to ss. The unit of each of the covariate in entries in every column of the covariate matrix $\mathbf{X}$ is the unit of it's its measurement or if it is standardized (e.g. subtract a covariate by its mean and divide by its standard deviation) then it is unitless(for . For further discussion on standardization and normalization see Gelman and Hill, 2006). The units of $\beta_{(p,1)}$ $(p \times 1)$ vector $\boldsymbol{\beta}$ are such that $\mathbf{X}\beta$ and s $\mathbf{X}\boldsymbol{\beta}$ and $\mathbf{s}$ have the same units. $\mathbf{Q}_{(m,m)}$ with units The prior error covariance matrix $\mathbf{Q}$ is an $(m \times m)$ matrix that represents the errors between $\mathbf{s}$ and $\mathbf{X}\boldsymbol{\beta}$ with unit of the entries being $\left(\mu\text{moles m}^{-2}\text{sec}^{-1}\right)^2$ describes errors between unknown s and $\mathbf{X}\beta$.

The analytical solutions for the unknown fluxes s $\mathbf{s}$ in the Bayesian case (denoted by the subscript B) and the geostatistical case (denoted by the subscript G) can be obtained from equations 11 and 12 Eq. (11) and (12) as given below.

$$\hat{\mathbf{s}}_B = \mathbf{s}_{\text{prior}}\mathbf{s}_{\text{prior}} + \mathbf{QH}^T\,\mathbf{QH}^t\left(\mathbf{HQH}^T\mathbf{HQH}^t + \mathbf{RR}\right)^{-1}\left(\mathbf{zz} - \mathbf{Hs}_{\text{prior}}\mathbf{Hs}_{\text{prior}}\right) \tag{11}$$

$$\hat{\mathbf{s}}_G = \mathbf{X}\,\mathbf{X}\boldsymbol{\beta} + \mathbf{QH}^T\,\mathbf{QH}^t\left(\mathbf{HQH}^T\mathbf{HQH}^t + \mathbf{RR}\right)^{-1}\left(\mathbf{zz} - \mathbf{HX}\beta\mathbf{HX}\boldsymbol{\beta}\right) \tag{12}$$

Equation 12 Eq. (12) is often expressed as $\mathbf{s}_G = \mathbf{X}\beta + \epsilon$ where $\mathbf{X}\beta$ $\mathbf{s}_G = \mathbf{X}\boldsymbol{\beta} + \boldsymbol{\epsilon}$ where $\mathbf{X}\boldsymbol{\beta}$ is the mean and $\epsilon = \mathbf{QH}^T\left(\mathbf{HQH}^T + \mathbf{R}\right)^{-1}$ $\boldsymbol{\epsilon} = \mathbf{QH}^t\left(\mathbf{HQH}^t + \mathbf{R}\right)^{-1}(\mathbf{z} - \mathbf{HX}\boldsymbol{\beta})$ is the stochastic part of the estimated fluxes. As the estimate of $\mathbf{s}_G$ in equation 12 $\mathbf{s}_G$ in Eq. (12) depends on the unknown $\beta\boldsymbol{\beta}$, it needs to be estimated prior to obtaining $\hat{\mathbf{s}}_G\hat{\mathbf{s}}_G$. The solution for the $\hat{\beta}\,\hat{\boldsymbol{\beta}}$ can be obtained from pre-determined quantities as described earlier in the context of equation 10 Eq. (10) and can be given as:

$$\hat{\boldsymbol{\beta}} = \mathbf{HX}^T\mathbf{HQH}^T + \mathbf{R}\boldsymbol{\Omega}^{-1}\mathbf{HX}\mathbf{A}^t\boldsymbol{\Psi}^{-1}\mathbf{HX}^T\,\mathbf{HQH}^T + \mathbf{R}^{-1}\mathbf{zz} \tag{13}$$

Plugging in $\hat{\boldsymbol{\beta}}$ in equation 12 leads to equation 14 Eq. (12) leads to Eq. (14) where all symbols are defined previously or in equation 15Eq. (15).

$$\hat{\mathbf{s}}_G = \mathbf{X}\mathbf{X}\boldsymbol{\Omega}^{-1}\mathbf{A}^T\mathbf{A}^t\boldsymbol{\Psi}^{-1}\mathbf{zz} + \mathbf{QH}^T\mathbf{QH}^t\boldsymbol{\Psi}^{-1}\left(\mathbf{zz} - \mathbf{AA}\boldsymbol{\Omega}^{-1}\mathbf{A}^T\mathbf{A}^t\boldsymbol{\Psi}^{-1}\mathbf{zz}\right) \quad \text{where} \tag{14}$$

$$\mathbf{AA} = \mathbf{HXHX}, \boldsymbol{\Psi}\boldsymbol{\Psi} = \left(\mathbf{HQH}^T\mathbf{HQH}^t + \mathbf{RR}\right), \boldsymbol{\Omega}\boldsymbol{\Omega} = \left(\mathbf{HXHX}\right)^{T\,t}\left(\mathbf{HQH}^T\mathbf{HQH}^t + \mathbf{RR}\right)^{-1}\mathbf{HX}^{-1}\mathbf{HX} \tag{15}$$

We differentiate equation 11 Note that, $\hat{\mathbf{s}}_B$ and $\hat{\mathbf{s}}_G$ in Eq. (11) and (12) are essentially functions which are represented by equations. This is a commonly adopted nomenclature that is used by researchers working in the field of atmospheric inversions. We differentiate Eq. (11) with respect to $\mathbf{s}_{\text{prior}}$, $\mathbf{R}$, $\mathbf{Q}$, $\mathbf{z}$ and equation 14 Eq. (14) with respect to $\mathbf{X}$, $\mathbf{R}$, $\mathbf{Q}$, $\mathbf{z}$ to obtain the local sensitivities. There are two ways to differentiate $\hat{\mathbf{s}}$ with respect to $\mathbf{z}$, $\mathbf{X}$, $\mathbf{H}$, $\mathbf{Q}$, and $\mathbf{R}$. In the first case, every entry in $\mathbf{z}$, $\mathbf{X}$, $\mathbf{H}$, $\mathbf{Q}$, and $\mathbf{R}$ can be considered as a parameter that results in differentiation of $\hat{\mathbf{s}}$ with respect to these quantities. On the other hand, if the structures of the covariance matrices $\mathbf{Q}$ and $\mathbf{R}$ are determined by parameters then $\hat{\mathbf{s}}$ can be differentiated just with

respect to these parameters. In the former case, ~~equations 11 and 14~~ Eq. (11) and (14) are used to differentiate $\hat{\mathbf{s}}$ with respect to an entry at a time in $\mathbf{z}$, $\mathbf{X}$, $\mathbf{H}$, $\mathbf{Q}$, and $\mathbf{R}$. Such an approach of entry-by-entry differentiation ~~that is one at a time differentiation is~~ is useful if the computational cost in terms of memory constraint is important or if we would like to know the influence of a single entry on $\hat{\mathbf{s}}$. We provide both sets of equations in this work.

3.2.1 ~~Local sensitivity analysis~~ LSA with respect to observations, priors, scaling factors, and ~~footprints~~forward operators

Local sensitivity of $\hat{\mathbf{s}}$ with respect to observations ($\mathbf{z}$) can be given as

~~$\frac{\partial \hat{\mathbf{s}}_B}{\partial \mathbf{z}} = \mathbf{Q}\mathbf{H}^T\mathbf{\Psi}^{-1}$~~

~~$\frac{\partial \hat{\mathbf{s}}_G}{\partial \mathbf{z}} = \mathbf{X}\mathbf{\Omega}^{-1}\mathbf{A}^{\mathbf{T}}\mathbf{\Psi}^{-1} + \mathbf{Q}\mathbf{H}^T\mathbf{\Psi}^{-1} - \mathbf{Q}\mathbf{H}^T\mathbf{\Psi}^{-1}\mathbf{A}\mathbf{\Omega}^{-1}\mathbf{A}^{\mathbf{T}}\mathbf{\Psi}^{-1} = \mathbf{A}$~~

$$\frac{\partial \hat{\mathbf{s}}_B}{\partial \mathbf{z}} = \mathbf{Q}\mathbf{H}^t\mathbf{\Psi}^{-1} \tag{16}$$

$$\frac{\partial \hat{\mathbf{s}}_G}{\partial \mathbf{z}} = \mathbf{X}\mathbf{\Omega}^{-1}\mathbf{A}^t\mathbf{\Psi}^{-1} + \mathbf{Q}\mathbf{H}^t\mathbf{\Psi}^{-1} - \mathbf{Q}\mathbf{H}^t\mathbf{\Psi}^{-1}\mathbf{A}\mathbf{\Omega}^{-1}\mathbf{A}^t\mathbf{\Psi}^{-1} \tag{17}$$

where all quantities are as defined earlier. ~~In the geostatistical case, equation 17 is also referred as **A** (for e.g. see Michalak et al., 2004 and Gourdji et al., 2010).~~ The units of $\frac{\partial \hat{\mathbf{s}}}{\partial \mathbf{z}}$ the entries in $\frac{\partial \hat{\mathbf{s}}}{\partial \mathbf{z}}$ are $\mu\text{moles}^{-1}\text{m}^2\text{sec}^{-1}\text{ppm}^{-1}$ ~~, which is~~ and the matrices are of dimension $(m \times n)$. These units are inverse of the units of $\mathbf{H}$. Local sensitivities with respect to an observation z_i for both the Bayesian and the geostatistical case can be written as vector of sensitivities times an indicator for the ~~i~~$^{\text{th}}$ i^{th} entry i.e. $\frac{\partial \hat{\mathbf{s}}}{\partial \mathbf{z}} e_i$ ~~where $e_i = \frac{\partial \mathbf{z}}{\partial z_i}$~~ $\frac{\partial \hat{\mathbf{s}}}{\partial \mathbf{z}} \mathbf{e}_i$ where $\mathbf{e}_i = \frac{\partial \mathbf{z}}{\partial z_i}$ is a vector of zeros with the ~~i~~$^{\text{th}}$ i^{th} entry equals to 1.

Note by utilizing $\frac{\partial \hat{\mathbf{s}}}{\partial \mathbf{z}} \frac{\partial \hat{\mathbf{s}}}{\partial \mathbf{z}}$, we can also obtain an averaging kernel (or model resolution matrix) and DOFS (see Rodgers, 2000). The averaging kernel matrix for any linear inverse model can be written as:

$$\text{~~Avk~~}\mathbf{V} = \frac{\partial \hat{\mathbf{s}}}{\partial \mathbf{z}} \frac{\partial \hat{\mathbf{s}}}{\partial \mathbf{z}} \times \mathbf{H} \quad \text{DOFS} = \text{Tr}\,\text{~~Avk~~}\mathbf{H} \tag{18}$$

where ~~Avk~~ $\mathbf{V}$ of dimension $(m \times m)$, is the local sensitivity of ~~$\hat{\mathbf{s}}$~~ $\hat{\mathbf{s}}$ with respect to the true unknown fluxes~~and DOFS~~. Then the DOFS can be computed by taking the trace of the averaging kernel matrix $\mathbf{V}$. DOFS represents the amount of information resolved by an inverse model when a set of observations have been assimilated (for a detailed discussion, see Rodgers, 2000 and Brasseur and Jacob, 2017). Theoretically, the value of DOFS cannot exceed number of observations (~~n~~n) in case of an underdetermined system and the number of fluxes (~~m~~m) in case of an overdetermined system.

We can directly compute local sensitivity of $\hat{\mathbf{s}}$ with respect to the prior mean flux $\mathbf{s}_{\text{prior}}$ in the Bayesian case. In the geostatistical case, the prior mean is modeled by two quantities $\mathbf{X}$ and ~~β~~$\boldsymbol{\beta}$. In this scenario, we need to find sensitivities with respect to $\mathbf{X}$ as well as ~~β~~$\boldsymbol{\beta}$. These local sensitivities ~~are given by~~can be given as:

$$\frac{\partial \hat{\mathbf{s}}_B}{\partial \mathbf{s}_{\text{prior}}} \frac{\partial \hat{\mathbf{s}}_B}{\partial \mathbf{s}_{\text{prior}}} = \mathbf{II} - \mathbf{CHCH} \tag{19}$$

$$\frac{\partial \hat{\mathbf{s}}_G}{\partial \mathbf{X}} \frac{\partial \hat{\mathbf{s}}_G}{\partial \mathbf{X}} = \mathbf{K}\mathbf{K}_z \otimes \left(\mathbf{II} + \left(\mathbf{M}\mathbf{A}^T\mathbf{M}\mathbf{A}^t - \mathbf{X}\boldsymbol{\Omega}\mathbf{X}\boldsymbol{\Omega}^{-1}\mathbf{A}\mathbf{A}^{Tt} - \mathbf{Q}\mathbf{H}^T\mathbf{Q}\mathbf{H}^t \right) \boldsymbol{\Psi}\boldsymbol{\Psi}^{-1}\mathbf{H}\mathbf{H} \right) + \left(\mathbf{X}\boldsymbol{\Omega}\mathbf{X}\boldsymbol{\Omega}^{-1} - \mathbf{M}\mathbf{M} \right) \otimes \left(\mathbf{F}\mathbf{F}_z - \mathbf{K}_z \right. \tag{20}$$

$$\frac{\partial \hat{\mathbf{s}}_G}{\partial \hat{\beta}} \frac{\partial \hat{\mathbf{s}}_G}{\partial \hat{\boldsymbol{\beta}}} = \mathbf{X}\mathbf{X} - \mathbf{C}\mathbf{A}\mathbf{C}\mathbf{A} \tag{21}$$

where ~~$\mathbf{A} = \mathbf{HX}, \mathbf{B} = \mathbf{Q}\mathbf{H}^T, \mathbf{C} = \mathbf{B}\boldsymbol{\Psi}^{-1}, \boldsymbol{\Omega} = \mathbf{A}^T\boldsymbol{\Psi}^{-1}\mathbf{A}, \mathbf{K}_z = \mathbf{z}^T\boldsymbol{\Psi}^{-1}\mathbf{A}\boldsymbol{\Omega}^{-1}, \mathbf{M} = \mathbf{C}\mathbf{A}\boldsymbol{\Omega}^{-1}$~~, and ~~$\mathbf{F}_z = \mathbf{z}^T\boldsymbol{\Psi}^{-1}\mathbf{H}$~~$\mathbf{A} = \mathbf{HX}$, $\mathbf{B} = \mathbf{Q}\mathbf{H}^t$, $\mathbf{C} = \mathbf{B}\boldsymbol{\Psi}^{-1}$, $\boldsymbol{\Omega} = \mathbf{A}^t\boldsymbol{\Psi}^{-1}\mathbf{A}$, $\mathbf{K}_z = \mathbf{z}^t\boldsymbol{\Psi}^{-1}\mathbf{A}\boldsymbol{\Omega}^{-1}$, $\mathbf{M} = \mathbf{C}\mathbf{A}\boldsymbol{\Omega}^{-1}$, and $\mathbf{F}_z = \mathbf{z}^t\boldsymbol{\Psi}^{-1}\mathbf{H}$. The symbol $\otimes$ represents the Kronecker product. The quantity ~~$\frac{\partial \hat{\mathbf{s}}_B}{\partial \mathbf{s}_{\text{prior}}}$ is unitless whereas the units of~~ $\frac{\partial \hat{\mathbf{s}}_B}{\partial \mathbf{s}_{\text{prior}}}$ is of dimension $(m \times m)$ and its entries are unitless. The quantity $\frac{\partial \hat{\mathbf{s}}_G}{\partial \hat{\boldsymbol{\beta}}}$ is of dimension $(m \times p)$ and units of the entries in each column of $\frac{\partial \hat{\mathbf{s}}_G}{\partial \hat{\beta}}$ is $\frac{\partial \hat{\mathbf{s}}_G}{\partial \hat{\boldsymbol{\beta}}}$ are of the form $(\mu\text{moles}^{-1}\text{m}^2\text{sec}^{-1})(\text{unit of } \beta_i)^{-1}$. The sensitivity matrix $\frac{\partial \hat{\mathbf{s}}_G}{\partial \mathbf{X}} \frac{\partial \hat{\mathbf{s}}_G}{\partial \mathbf{X}}$ is of dimension ~~$m \times mp$ where every i$^{\text{th}}$~~ $(m \times mp)$ where every i^{th} block of m columns $((i-1)m + A : im)$ of $\frac{\partial \hat{\mathbf{s}}_G}{\partial \mathbf{X}} \frac{\partial \hat{\mathbf{s}}_G}{\partial \mathbf{X}}$ has units of the form ~~$(\mu\text{moles}^{-1}\text{m}^2\text{sec}^{-1})(\text{unit of } \mathbf{X}_i)^{-1}$ where $\mathbf{X}_i$ is the i$^{\text{th}}$~~ $(\mu\text{moles}^{-1}\text{m}^2\text{sec}^{-1})(\text{unit of } \mathbf{X}_i)^{-1}$ where $\mathbf{X}_i$ is the i^{th} column of $\mathbf{X}$. Note that, the sensitivity matrix $\frac{\partial \hat{\mathbf{s}}_B}{\partial \mathbf{s}_{\text{prior}}}$ in Eq. (19) can also be thought as proportion of posterior uncertainty to that of the prior uncertainty. In context of the Bayesian case, proportional uncertainty reduction becomes averaging kernel.

Sometimes, it is important to know the influence of the prior of any particular grid point or an area consisting of few points on $\hat{\mathbf{s}}$. Local ~~sensitivities~~ sensitivity of $\hat{\mathbf{s}}$ with respect to the ~~i$^{\text{th}}$ entry in $\mathbf{s}_{\text{prior}}$~~ i^{th} entry in $\mathbf{s}_{\text{prior}}$ and $\hat{\beta}_i$ ~~are straightforward~~ is a matrix of dimension $(m \times 1)$ and can be written as $\frac{\partial \hat{\mathbf{s}}_B}{\partial \mathbf{s}_{\text{prior}}} e_i$ ~~and~~ $\frac{\partial \hat{\mathbf{s}}_G}{\partial \hat{\beta}} e_i$ $\frac{\partial \hat{\mathbf{s}}_B}{\partial \mathbf{s}_{\text{prior}}} \mathbf{e}_i$ and $\frac{\partial \hat{\mathbf{s}}_G}{\partial \hat{\boldsymbol{\beta}}} \mathbf{e}_i$ respectively. However, the entry-wise $\frac{\partial \hat{\mathbf{s}}_G}{\partial \mathbf{X}_{ij}} \frac{\partial \hat{\mathbf{s}}_G}{\partial \mathbf{X}_{ij}}$ is more complex and can be given by:

$$\frac{\partial \hat{\mathbf{s}}_G}{\partial \mathbf{X}_{ij}} \frac{\partial \hat{\mathbf{s}}_G}{\partial X_{ij}} = (\mathbf{II} - \mathbf{CHCH}) \left(\left(\mathbf{II} - \mathbf{X}\boldsymbol{\Omega}\mathbf{X}\boldsymbol{\Omega}^{-1}\mathbf{X}^T\mathbf{H}^T\mathbf{X}^t\mathbf{H}^t\boldsymbol{\Psi}^{-1}\mathbf{H}\mathbf{H} \right) \frac{\partial \mathbf{X}}{\partial \mathbf{X}_{ij}} \frac{\partial \mathbf{X}}{\partial \mathbf{X}_{ij}} \boldsymbol{\Omega}\boldsymbol{\Omega}^{-1}\mathbf{X}^T\mathbf{X}^t + \mathbf{X}\boldsymbol{\Omega}\mathbf{X}\boldsymbol{\Omega}^{-1} \frac{\partial \mathbf{X}^T}{\partial \mathbf{X}_{ij}} \frac{\partial \mathbf{X}^t}{\partial \mathbf{X}_{ij}} \left(\mathbf{II} - \mathbf{H}^T \right. \right. \tag{22}$$

where ~~$\frac{\partial \mathbf{X}^T}{\partial \mathbf{X}_{ij}} = E_{ij}$ $\frac{\partial \mathbf{X}^t}{\partial \mathbf{X}_{ij}} = \mathbf{E}_{ij}$~~ is a single-entry matrix with a one for a X_{ij} for which differentiation is being performed and zero everywhere else. For $\mathbf{z}$, entry-by-entry differentiation can be easily performed, since both ~~equations 11 and 14~~ Eq. (11) and (14) result from linear models and are functions of the form ~~$\boldsymbol{\Phi}\mathbf{z} + \mathbf{n}$ where $\boldsymbol{\Phi}$ and $\mathbf{n}$~~ $\boldsymbol{\Phi}\mathbf{z} + \mathbf{n}$ where $\boldsymbol{\Phi}$ and $\mathbf{n}$ are independent of ~~$\mathbf{z}\mathbf{z}$~~. For example, ~~$\boldsymbol{\Phi}$ and $\mathbf{n}$ for equation 11 are $\mathbf{Q}\mathbf{H}^T\left(\mathbf{H}\mathbf{Q}\mathbf{H}^T + \mathbf{R}\right)^{-1}$ and $\mathbf{s}_{\text{prior}} - \mathbf{Q}\mathbf{H}^T\left(\mathbf{H}\mathbf{Q}\mathbf{H}^T + \mathbf{R}\right)^{-1}\mathbf{H}\mathbf{s}_{\text{prior}}$~~ $\boldsymbol{\Phi}$ and $\mathbf{n}$ for Eq. (11) are $\mathbf{Q}\mathbf{H}^t\left(\mathbf{H}\mathbf{Q}\mathbf{H}^t + \mathbf{R}\right)^{-1}$ and $\mathbf{s}_{\text{prior}} - \mathbf{Q}\mathbf{H}^t\left(\mathbf{H}\mathbf{Q}\mathbf{H}^t + \mathbf{R}\right)^{-1}\mathbf{H}\mathbf{s}_{\text{prior}}$ respectively and are independent of ~~$\mathbf{z}\mathbf{z}$~~. In

this case, $\frac{\partial \hat{\mathbf{s}}_B}{\partial \mathbf{z}_i}\frac{\partial \hat{\mathbf{s}}_B}{\partial z_i}$ can be written as $\mathbf{\Phi e_i}\,\mathbf{\Phi e_i}$ where $\boldsymbol{e_i}$ is a single-entry vector with a one for a $\boldsymbol{z}_i$ for which differentiation is being performed and zero everywhere else. $\frac{\partial \hat{\mathbf{s}}_G}{\partial \mathbf{z}_i}$ Local sensitivity $\frac{\partial \hat{\mathbf{s}}_G}{\partial z_i}$ can similarly be defined for the respective ~~$\mathbf{\Phi}$.~~ $\mathbf{\Phi}$. Here both the quantities $\frac{\partial \hat{\mathbf{s}}_G}{\partial X_{ij}}$ and $\frac{\partial \hat{\mathbf{s}}_B}{\partial z_i}$ are matrices of dimension $(m \times 1)$.

Local sensitivity of $\hat{\mathbf{s}}$ with respect to ~~a~~ an entry in the forward operator has units of the form $\left(\mu\text{moles}^{-1}\text{m}^2\text{sec}^{-1}\right)^2\text{ppm}^{-1}$. In the Bayesian case this sensitivity can be written as:

$$\frac{\partial \hat{\mathbf{s}}_B}{\partial \mathbf{H}}\frac{\partial \hat{\mathbf{s}}_B}{\partial \mathbf{H}} = \mathbf{QQ}\otimes\mathbf{PP}_z - \mathbf{BP}\mathbf{BP}_z\otimes\mathbf{C}^T\mathbf{C}^t - \mathbf{BC}^T\mathbf{BC}^t\otimes\mathbf{PP}_z - \mathbf{QQ}\otimes\mathbf{DD} + \mathbf{BD}\mathbf{BD}\otimes\mathbf{C}^T\mathbf{C}^t + \mathbf{BC}^T\mathbf{BC}^t\otimes\mathbf{DD} - \mathbf{ss}_{\text{prior}}\otimes\mathbf{C}^T \tag{23}$$

where $\frac{\partial \hat{\mathbf{s}}_B}{\partial \mathbf{H}}$ is a sensitivity matrix of dimension $(m \times mn)$. In the geostatistical case, this sensitivity can be partitioned into two components i.e., $\frac{\partial \hat{\beta}}{\partial \mathbf{H}}$ ~~and~~ $\frac{\partial \hat{\epsilon}}{\partial \mathbf{H}}$ $\frac{\partial \hat{\boldsymbol{\beta}}}{\partial \mathbf{H}}$ and $\frac{\partial \hat{\boldsymbol{\epsilon}}}{\partial \mathbf{H}}$ as shown in ~~equation 24 where~~ $\frac{\partial \hat{\beta}}{\partial \mathbf{H}}$ ~~and~~ $\frac{\partial \hat{\epsilon}}{\partial \mathbf{H}}$ Eq. (24) where $\frac{\partial \hat{\boldsymbol{\beta}}}{\partial \mathbf{H}}$ and $\frac{\partial \hat{\boldsymbol{\epsilon}}}{\partial \mathbf{H}}$ are obtained in an orderly sequence from ~~equations 25 and 26~~Eq. (25) and (26).

$$\frac{\partial \hat{\mathbf{s}}_G}{\partial \mathbf{H}}\frac{\partial \hat{\mathbf{s}}_G}{\partial \mathbf{H}} = \mathbf{X}\frac{\partial \hat{\beta}}{\partial \mathbf{H}}\mathbf{X}\frac{\partial \hat{\boldsymbol{\beta}}}{\partial \mathbf{H}} + \frac{\partial \hat{\epsilon}}{\partial \mathbf{H}}\frac{\partial \hat{\boldsymbol{\epsilon}}}{\partial \mathbf{H}} \quad \text{where} \tag{24}$$

$$\frac{\partial \hat{\beta}}{\partial \mathbf{H}}\frac{\partial \hat{\boldsymbol{\beta}}}{\partial \mathbf{H}} = -\mathbf{LL}\otimes\mathbf{GG}_z - \mathbf{PP}_z{}^T\mathbf{A}\boldsymbol{\Omega}^t\mathbf{A}\boldsymbol{\Omega}^{-1}\mathbf{X}^T\mathbf{X}^t\otimes\mathbf{KK}^T + \mathbf{GG}_z\mathbf{HQ}\mathbf{HQ}\otimes\mathbf{K}^T\mathbf{K}^t + \mathbf{NN}\otimes\mathbf{GG}_z + \mathbf{LL}\otimes\mathbf{PP}_z^T - \mathbf{PP}_z^T\mathbf{HQ}\mathbf{HQ} \tag{25}$$

$$\frac{\partial \hat{\epsilon}}{\partial \mathbf{H}}\frac{\partial \hat{\boldsymbol{\epsilon}}}{\partial \mathbf{H}} = \mathbf{QQ}\otimes\mathbf{PP}_z - \mathbf{Cz}\mathbf{Cz}\otimes\mathbf{C}^T\mathbf{C}^t - \mathbf{CHQ}\mathbf{CHQ}\otimes\mathbf{PP}_z - \mathbf{XK}^T\mathbf{z}\mathbf{XK}^t\mathbf{z}\otimes\mathbf{CC}^T - \mathbf{CA}\frac{\partial \hat{\beta}}{\partial \mathbf{H}}\mathbf{CA}\frac{\partial \hat{\boldsymbol{\beta}}}{\partial \mathbf{H}} \tag{26}$$

The expanded form of some of the symbols in ~~equations 23 through 26, those~~ Eq. (23) through (26), which have not been expanded yet can be written as ~~$\mathbf{D} = \mathbf{\Psi H s}_{\text{prior}}$, $\mathbf{G}_z = \mathbf{z}^T\mathbf{\Psi}^{-1}\mathbf{A}\Omega^{-1}\mathbf{A}^T\mathbf{\Psi}^{-1}$, $\mathbf{L} = \mathbf{\Omega}^{-1}\mathbf{X}^T$, $\mathbf{N} = \mathbf{\Omega}^{-1}\mathbf{A}^T\mathbf{\Psi}^{-1}\mathbf{HQ}$, $\mathbf{P}_z = \mathbf{\Psi}^{-1}\mathbf{z}$, and $\mathbf{K} = \mathbf{\Psi}^{-1}\mathbf{A}\Omega^{-1}$. The unit of~~ $\frac{\partial \hat{\mathbf{s}}}{\partial \mathbf{H}}$ ~~is~~ $\mathbf{D} = \mathbf{\Psi H s}_{\text{prior}}$, $\mathbf{G}_z = \mathbf{z}^t\mathbf{\Psi}^{-1}\mathbf{A}\Omega^{-1}\mathbf{A}^t\mathbf{\Psi}^{-1}$, $\mathbf{L} = \mathbf{\Omega}^{-1}\mathbf{X}^t$, $\mathbf{N} = \mathbf{\Omega}^{-1}\mathbf{A}^t\mathbf{\Psi}^{-1}\mathbf{HQ}$, $\mathbf{P}_z = \mathbf{\Psi}^{-1}\mathbf{z}$, and $\mathbf{K} = \mathbf{\Psi}^{-1}\mathbf{A}\Omega^{-1}$. The quantities $\frac{\partial \hat{\mathbf{s}}_G}{\partial \mathbf{H}}$, $\frac{\partial \hat{\boldsymbol{\beta}}}{\partial \mathbf{H}}$, and $\frac{\partial \hat{\boldsymbol{\epsilon}}}{\partial \mathbf{H}}$ are sensitivity matrices of dimensions $(m \times mn)$, $(p \times mn)$, and $(m \times mn)$ respectively. The units of the entries of $\frac{\partial \hat{\mathbf{s}}}{\partial \mathbf{H}}$ are of the form $(\mu\text{moles}^{-1}\text{m}^2\text{sec}^{-1})^2\text{ppm}^{-1}$.

There might be times when we would like to know the sensitivity of the transport (~~H~~$\mathbf{H}$) with respect to certain source locations only. In this case, we can use ~~ij form of equations 23 through 26 to obtain~~ $\frac{\partial \hat{\mathbf{s}}_B}{\partial H_{ij}}$ ij form of Eq. (23) through (26) to obtain $\frac{\partial \hat{\mathbf{s}}_B}{\partial H_{ij}}$ in parts. In this formulation $\frac{\partial \hat{\mathbf{s}}_B}{\partial H_{ij}}$, $\frac{\partial \hat{\mathbf{s}}_B}{\partial H_{ij}}$ can be given as:

$$\frac{\partial \hat{\mathbf{s}}_B}{\partial H_{ij}}\frac{\partial \hat{\mathbf{s}}_B}{\partial H_{ij}} = \mathbf{C}\frac{\partial \mathbf{H}}{\partial \mathbf{H}_{ij}}\mathbf{C}\frac{\partial \mathbf{H}}{\partial H_{ij}}\left(\mathbf{C}\mathbf{C}(\mathbf{H}\mathbf{s}\mathbf{H}\mathbf{s}_{\text{prior}} - \mathbf{z}\mathbf{z}) - \mathbf{s}\mathbf{s}_{\text{prior}}\right) + (\mathbf{Q}\mathbf{Q} - \mathbf{C}\mathbf{H}\mathbf{Q}\mathbf{C}\mathbf{H}\mathbf{Q})\left(\frac{\partial \mathbf{H}}{\partial H_{ij}}\frac{\partial \mathbf{H}}{\partial H_{ij}}\right)^{T}\mathbf{H}^{t}\mathbf{\Psi}\mathbf{\Psi}^{-1}(\mathbf{z}\mathbf{z} - \mathbf{H}\mathbf{s}\mathbf{H}\mathbf{s}_{\text{prior}}) \tag{27}$$

$$\frac{\partial \hat{\mathbf{s}}_G}{\partial H_{ij}}\frac{\partial \hat{\mathbf{s}}_G}{\partial H_{ij}} = \mathbf{X}\frac{\partial \hat{\beta}}{\partial H_{ij}}\mathbf{X}\frac{\partial \hat{\boldsymbol{\beta}}}{\partial H_{ij}} + \frac{\partial \hat{\epsilon}}{\partial H_{ij}}\frac{\partial \hat{\boldsymbol{\epsilon}}}{\partial H_{ij}}, \quad \text{where} \tag{28}$$

$$\frac{\partial \hat{\beta}}{\partial H_{ij}}\frac{\partial \hat{\boldsymbol{\beta}}}{\partial H_{ij}} = \left(-\mathbf{K}^{T}\frac{\partial \mathbf{H}}{\partial H_{ij}}\mathbf{K}^{t}\frac{\partial \mathbf{H}}{\partial H_{ij}}\left(\mathbf{X}\mathbf{N}\mathbf{X}\mathbf{N} - \mathbf{C}\mathbf{A}\mathbf{S}\mathbf{C}\mathbf{A}\mathbf{S} + \mathbf{Q}\mathbf{H}^{T}\mathbf{Q}\mathbf{H}^{t}\right) + \mathbf{K}^{T}\mathbf{H}\mathbf{Q}\frac{\partial \mathbf{H}^{T}}{\partial H_{ij}}\mathbf{K}^{t}\mathbf{H}\mathbf{Q}\frac{\partial \mathbf{H}^{t}}{\partial H_{ij}}\left(\mathbf{\Psi}\mathbf{\Psi}^{-1}\mathbf{A}\mathbf{S}^{T}\mathbf{A}\mathbf{S}^{t} - \mathbf{I}\mathbf{I}\right) + \tag{29}$$

$$\frac{\partial \hat{\epsilon}}{\partial H_{ij}}\frac{\partial \hat{\boldsymbol{\epsilon}}}{\partial H_{ij}} = \left(\mathbf{Q}\frac{\partial \mathbf{H}^{T}}{\partial H_{ij}}\mathbf{Q}\frac{\partial \mathbf{H}^{t}}{\partial H_{ij}} - \mathbf{C}\frac{\partial \mathbf{H}}{\partial H_{ij}}\mathbf{Q}\mathbf{H}^{T}\mathbf{C}\frac{\partial \mathbf{H}}{\partial H_{ij}}\mathbf{Q}\mathbf{H}^{t} - \mathbf{C}\mathbf{H}\mathbf{Q}\frac{\partial \mathbf{H}^{T}}{\partial H_{ij}}\mathbf{C}\mathbf{H}\mathbf{Q}\frac{\partial \mathbf{H}^{t}}{\partial H_{ij}}\right)\mathbf{\Psi}\mathbf{\Psi}^{-1}\left(\mathbf{z}\mathbf{z} - \mathbf{A}\mathbf{A}\hat{\boldsymbol{\beta}}\right) - \mathbf{C}\mathbf{C}\left(\frac{\partial \mathbf{H}}{\partial H_{ij}}\mathbf{X}\frac{\partial \mathbf{H}}{\partial H_{ij}} \tag{30}$$

where ~~$\mathbf{S} = \mathbf{A}\mathbf{\Omega}^{-1}$~~ $\mathbf{S} = \mathbf{A}\mathbf{\Omega}^{-1}$ and the matrix $\frac{\partial \mathbf{H}}{\partial H_{ij}}\frac{\partial \mathbf{H}}{\partial H_{ij}}$ is a single-entry matrix with a one for a H_{ij} entry for which the differentiation is being performed and zero everywhere else. ~~Units of $\frac{\partial \hat{\mathbf{s}}_B}{\partial H_{ij}}$ and $\frac{\partial \hat{\mathbf{s}}_G}{\partial H_{ij}}$~~ The quantities $\frac{\partial \hat{\mathbf{s}}_B}{\partial H_{ij}}$, $\frac{\partial \hat{\mathbf{s}}_G}{\partial H_{ij}}$, $\frac{\partial \hat{\boldsymbol{\beta}}}{\partial H_{ij}}$, and $\frac{\partial \hat{\boldsymbol{\epsilon}}}{\partial H_{ij}}$ are sensitivity matrices of dimensions $(m \times 1)$, $(m \times 1)$, $(p \times 1)$, and $(m \times 1)$ respectively. Units of $\frac{\partial \hat{\mathbf{s}}_B}{\partial H_{ij}}$ and $\frac{\partial \hat{\mathbf{s}}_G}{\partial H_{ij}}$ are the same as their kronecker product counterparts.

3.2.2 ~~Local sensitivity analysis~~ LSA with respect to error covariance matrices and prior information

In order to compute the local sensitivities of $\hat{\mathbf{s}}$ with respect to $\mathbf{Q}$ and $\mathbf{R}$, consider that they are parametrized as ~~$\mathbf{Q}(\theta_{\mathbf{Q}})$ and $\mathbf{R}(\theta_{\mathbf{R}})$ where $\theta_{\mathbf{Q}}$ and $\theta_{\mathbf{R}}$~~ $\mathbf{Q}(\boldsymbol{\theta}_{\mathbf{Q}})$ and $\mathbf{R}(\boldsymbol{\theta}_{\mathbf{R}})$ where $\boldsymbol{\theta}_{\mathbf{Q}}$ and $\boldsymbol{\theta}_{\mathbf{R}}$ are the parameter vectors. The differentiation with respect to error covariance parameters in $\mathbf{Q}$ and $\mathbf{R}$ can be accomplished ~~through equations 31 through 34~~ from Eq. (31) through (34) where the subscript i indicates the i^{th} covariance parameter for which differentiation is being performed.

$$\frac{\partial \hat{\mathbf{s}}_B}{\partial \theta_{Q_i}}\frac{\partial \hat{\mathbf{s}}_B}{\partial \theta_{Q_i}} = \left(\mathbf{I}\mathbf{I} - \mathbf{C}\mathbf{H}\mathbf{C}\mathbf{H}\right)\frac{\partial \mathbf{Q}}{\partial \theta_{Q_i}}\mathbf{H}^{T}\mathbf{\Psi}\frac{\partial \mathbf{Q}}{\partial \theta_{Q_i}}\mathbf{H}^{t}\mathbf{\Psi}^{-1}(\mathbf{z}\mathbf{z} - \mathbf{H}\mathbf{s}\mathbf{H}\mathbf{s}_{\text{prior}}) \tag{31}$$

$$\frac{\partial \hat{\mathbf{s}}_G}{\partial \theta_{Q_i}}\frac{\partial \hat{\mathbf{s}}_G}{\partial \theta_{Q_i}} = \left(-\mathbf{X}\mathbf{\Omega}\mathbf{X}\mathbf{\Omega}^{-1}\mathbf{A}\mathbf{A}^{T}\mathbf{\Psi}\mathbf{\Psi}^{-1}\mathbf{H}\mathbf{H} + \mathbf{I}\mathbf{I} - \mathbf{Q}\mathbf{H}\mathbf{Q}\mathbf{H}^{T}\mathbf{\Psi}\mathbf{\Psi}^{-1}\mathbf{H}\mathbf{H} + \mathbf{Q}\mathbf{H}\mathbf{Q}\mathbf{H}^{T}\mathbf{\Psi}\mathbf{\Psi}^{-1}\mathbf{A}\mathbf{\Omega}\mathbf{A}\mathbf{\Omega}^{-1}\mathbf{A}\mathbf{A}^{T}\mathbf{\Psi}\mathbf{\Psi}^{-1}\mathbf{H}\mathbf{H}\right)\frac{\partial \mathbf{Q}}{\partial \theta_{Q_i}}\mathbf{H} \tag{32}$$

$$\frac{\partial \hat{\mathbf{s}}_B}{\partial \theta_{R_i}}\frac{\partial \hat{\mathbf{s}}_B}{\partial \theta_{R_i}} = -\mathbf{C}\frac{\partial \mathbf{R}}{\partial \theta_{R_i}}\mathbf{\Psi}\mathbf{C}\frac{\partial \mathbf{R}}{\partial \theta_{R_i}}\mathbf{\Psi}^{-1}(\mathbf{z}\mathbf{z} - \mathbf{H}\mathbf{s}\mathbf{H}\mathbf{s}_{\text{prior}}) \tag{33}$$

$$\frac{\partial \hat{\mathbf{s}}_G}{\partial \theta_{R_i}}\frac{\partial \hat{\mathbf{s}}_G}{\partial \theta_{R_i}} = (-\mathbf{X}\mathbf{\Omega}\mathbf{X}\mathbf{\Omega}^{-1}\mathbf{A}\mathbf{A}^{T} - \mathbf{B}\mathbf{B} + \mathbf{C}\mathbf{A}\mathbf{\Omega}\mathbf{C}\mathbf{A}\mathbf{\Omega}^{-1}\mathbf{A}\mathbf{A}^{T})\mathbf{\Psi}\mathbf{\Psi}^{-1}\frac{\partial \mathbf{R}}{\partial \theta_{R_i}}\mathbf{\Psi}\frac{\partial \mathbf{R}}{\partial \theta_{R_i}}\mathbf{\Psi}^{-1}(\mathbf{z}\mathbf{z} - \mathbf{A}\mathbf{\Omega}\mathbf{A}\mathbf{\Omega}^{-1}\mathbf{A}\mathbf{A}^{T}\mathbf{\Psi}\mathbf{\Psi}^{-1}\mathbf{z}\mathbf{z}) \tag{34}$$

The units of $\frac{\partial \hat{\mathbf{s}}}{\partial \theta_{Q_i}}$ and $\frac{\partial \hat{\mathbf{s}}}{\partial \theta_{R_i}}$ All the quantities $\frac{\partial \hat{\mathbf{s}}_B}{\partial \theta_{Q_i}}$, $\frac{\partial \hat{\mathbf{s}}_G}{\partial \theta_{Q_i}}$, $\frac{\partial \hat{\mathbf{s}}_B}{\partial \theta_{R_i}}$, and $\frac{\partial \hat{\mathbf{s}}_G}{\partial \theta_{R_i}}$ are sensitivity matrices of dimension $(m \times 1)$ and the units of the entries of $\frac{\partial \hat{\mathbf{s}}}{\partial \theta_{Q_i}}$ and $\frac{\partial \hat{\mathbf{s}}}{\partial \theta_{R_i}}$ are of the form $(\mu\text{moles}^{-1}\text{m}^2\text{sec}^{-1})(\text{unit of } \theta_{Q_i} \text{ or } \theta_{R_i})^{-1}$. It is also possible to find $\frac{\partial \hat{\mathbf{s}}}{\partial \mathbf{Q}}$ and $\frac{\partial \hat{\mathbf{s}}}{\partial \mathbf{R}}$ $\frac{\partial \hat{\mathbf{s}}}{\partial \mathbf{Q}}$ and $\frac{\partial \hat{\mathbf{s}}}{\partial \mathbf{R}}$ directly as shown in equations 35 through 38Eq. (35) through (38).

$$\frac{\partial \hat{\mathbf{s}}_B}{\partial \mathbf{Q}} \frac{\partial \hat{\mathbf{s}}_B}{\partial \mathbf{Q}} = \mathbf{H}^T \mathbf{\Psi} \mathbf{H}^t \mathbf{\Psi}^{-1} (\mathbf{z}\mathbf{z} - \mathbf{H}\mathbf{s}\mathbf{H}\mathbf{s}_{\text{prior}}) \otimes \left(\mathbf{I}\mathbf{I} - \mathbf{H}^T \mathbf{\Psi} \mathbf{H}^t \mathbf{\Psi}^{-1} \mathbf{B}^T \mathbf{B}^t \right) \tag{35}$$

$$\frac{\partial \hat{\mathbf{s}}_G}{\partial \mathbf{Q}} \frac{\partial \hat{\mathbf{s}}_G}{\partial \mathbf{Q}} = \left(\mathbf{G}\mathbf{G}_z - \mathbf{z}^T \mathbf{z}^t \right) \mathbf{\Psi} \mathbf{\Psi}^{-1} \mathbf{H}\mathbf{H} \otimes \left(\left(\mathbf{B}\mathbf{B} - \mathbf{M}\mathbf{A}^T \mathbf{M}\mathbf{A}^t + \mathbf{L}^T \mathbf{A}^T \mathbf{L}^t \mathbf{A}^t \right) \mathbf{\Psi} \mathbf{\Psi}^{-1} \mathbf{H}\mathbf{H} - \mathbf{I}\mathbf{I} \right) \tag{36}$$

$$\frac{\partial \hat{\mathbf{s}}_B}{\partial \mathbf{R}} \frac{\partial \hat{\mathbf{s}}_B}{\partial \mathbf{R}} = \mathbf{\Psi} \mathbf{\Psi}^{-1} (\mathbf{z}\mathbf{z} - \mathbf{H}\mathbf{s}\mathbf{H}\mathbf{s}_{\text{prior}}) \otimes \mathbf{\Psi} \mathbf{\Psi}^{-1} \mathbf{H}\mathbf{Q}\mathbf{H}\mathbf{Q} \tag{37}$$

$$\frac{\partial \hat{\mathbf{s}}_G}{\partial \mathbf{R}} \frac{\partial \hat{\mathbf{s}}_G}{\partial \mathbf{R}} = \left(\mathbf{G}\mathbf{G}_z - \mathbf{z}^T \mathbf{z}^t \right) \mathbf{\Psi} \mathbf{\Psi}^{-1} \otimes \left(\mathbf{B}\mathbf{B} - \mathbf{M}\mathbf{A}^T \mathbf{M}\mathbf{A}^t + \mathbf{L}^T \mathbf{A}^T \mathbf{L}^t \mathbf{A}^t \right) \mathbf{\Psi} \mathbf{\Psi}^{-1} \tag{38}$$

Equations 35 through 38 First two quantities $\frac{\partial \hat{\mathbf{s}}_B}{\partial \mathbf{Q}}$ and $\frac{\partial \hat{\mathbf{s}}_G}{\partial \mathbf{Q}}$ are sensitivity matrices of dimension $(m \times m^2)$. The second set of quantities $\frac{\partial \hat{\mathbf{s}}_B}{\partial \mathbf{R}}$ and $\frac{\partial \hat{\mathbf{s}}_G}{\partial \mathbf{R}}$ are sensitivity matrices of dimension $(m \times n^2)$. Equations (35) through (38) are useful when ~~$\mathbf{Q}$ and $\mathbf{R}$~~ $\mathbf{Q}$ and $\mathbf{R}$ are fully or partially non-parametric. However, dimensions of these matrices can be quite large and users needs to be careful in realizing the full matrix.

3.3 ~~Global sensitivity analysis~~GSA: a variance-based approach

~~Global sensitivity analysis~~ GSA is a process of apportioning the uncertainty in an output estimate to the uncertainty in each input ~~parameters~~parameter. The term "global" stems from the idea of accounting for the effect of all input parameters simultaneously. This is different from "local" sensitivity analysis where the effect of a small change in each parameter on the functional output is ~~separately considered keeping everything else~~ considered separately while keeping all other parameters constant. Although quite important, a detailed ~~global sensitivity analysis is challenging due to it 's demand for the knowledge of~~ GSA is challenging as it requires knowledge of the probabilistic variations of all possible combinations (also known as covariance) of the input parameters. In atmospheric inverse problems, it is hard to know the joint variation of all input parameters. However, sometimes it might be possible to know the approximate joint variation of a small subset of input parameters (e.g. the covariance between $\mathbf{Q}$ and $\mathbf{R}$ parameters). In such case, we can use a variance based approximate method to find the relative contribution of their uncertainties with respect to the total flux uncertainty. Note it is also possible to use DGSM (see Sobol and Kucherenko, 2010) or the active-subspace technique (see Constantine and Diaz, 2017) in such a scenario. Since the variance based method proposed here doesn't require any sampling and can levearage previously computed derivatives, we adher to this method in this study as an easy extension after LSA.

The GSA method presented here leverages local sensitivities but actually belongs to the class of variance based methods. This is an approach that addresses the contribution to the total variance of the estimated fluxes. This is an approximate method unlike the exact decomposition technique of Sobol using conditional variances. It applies a simple first-order Taylor's approximation

around parameter estimates to obtain an approximate representation. This approach has been used in many research works including environmental modeling (e.g. Hamby, 1994) and life cycle assessment (Groen et al., 2017; Heijungs, 1996) among others.

Broadly, we can consider $\hat{\mathbf{s}}$ as a function of the ~~independent variables $\mathbf{Q}, \mathbf{R}, \mathbf{H}, \mathbf{X}(\text{or } \mathbf{s}_{\text{prior}})$, and $\mathbf{z}$~~ covariates $\mathbf{Q}, \mathbf{R}, \mathbf{H}, \mathbf{X}(\text{or } \mathbf{s}_{\text{prior}})$, and $\mathbf{z}$ i.e. ~~$\hat{\mathbf{s}} = f(\mathbf{Q}, \mathbf{R}, \mathbf{H}, \mathbf{X}(\text{or } \mathbf{s}_{\text{prior}}), \mathbf{z})$~~ $\hat{\mathbf{s}} = \mathbf{f}(\mathbf{Q}, \mathbf{R}, \mathbf{H}, \mathbf{X}(\text{or } \mathbf{s}_{\text{prior}}), \mathbf{z})$. We can then ~~see~~ compute how uncertainties of the individual components of ~~f~~ $\mathbf{f}$ are accounted in the overall uncertainty of $\hat{\mathbf{s}}$ ~~. We apply~~ by applying multivariate Taylor series expansion of ~~$\hat{\mathbf{s}}$ about it's~~ $\hat{\mathbf{s}}$ about its mean. Approximation up to first-order polynomial of the Taylor series expansion leads to the equation:

$$V_{\hat{\mathbf{s}}} \text{Var}(\hat{\mathbf{s}}) = \left(\frac{\partial \hat{\mathbf{s}}}{\partial \boldsymbol{\theta}} \frac{\partial \hat{\mathbf{s}}}{\partial \boldsymbol{\theta}}^T \mathbf{W}_\theta{}^t \mathbf{W}_{\boldsymbol{\theta}} \frac{\partial \hat{\mathbf{s}}}{\partial \boldsymbol{\theta}} \right)_{\boldsymbol{\theta}=\hat{\boldsymbol{\theta}}} + \text{Error}, \quad \text{where}$$

~~$\boldsymbol{\theta} = (\boldsymbol{\theta}_{\boldsymbol{Q}}, \boldsymbol{\theta}_{\boldsymbol{R}}, \boldsymbol{\theta}_{\boldsymbol{H}}, \theta_{\mathbf{X}}(\text{or } \mathbf{s}_{\text{prior}}), \boldsymbol{\theta}_{\boldsymbol{z}})$~~ $\boldsymbol{\theta} = (\boldsymbol{\theta}_{\boldsymbol{Q}}, \boldsymbol{\theta}_{\boldsymbol{R}}, \boldsymbol{\theta}_{\boldsymbol{H}}, \boldsymbol{\theta}_{\mathbf{X}}(\text{or } \mathbf{s}_{\text{prior}}), \boldsymbol{\theta}_{\boldsymbol{z}})$ is the vector of parameters and ~~$\mathbf{W} = \text{Var}(\boldsymbol{\theta})$~~ $\mathbf{W} = \text{Var}(\boldsymbol{\theta})$ is the covariance matrix of the parameters. It is however, challenging to estimate some of the individual covariance quantities such as the cross-covariance between $\boldsymbol{\theta}_{\boldsymbol{R}}$ and $\boldsymbol{\theta}_{\boldsymbol{H}}$ or between $\boldsymbol{\theta}_{\boldsymbol{H}}$, and $\boldsymbol{\theta}_{\boldsymbol{Q}}$ to get the best possible decomposition of the total uncertainty of $\hat{\mathbf{s}}$. Assuming no cross-covariance between $\mathbf{Q}$ and $\mathbf{R}$ and ignoring other parameters not related to the variance parameters, the diagonal of the variance of the posterior fluxes can be approximated as:

$$V_{\hat{s}_i} \text{Var}(\hat{s}_i) = \sum_{j=1}^{L} \left(\frac{\partial \hat{\mathbf{s}}}{\partial \boldsymbol{\theta}_{\boldsymbol{Q}}(j)} \frac{\partial \hat{\mathbf{s}}}{\partial \theta_{Q_j}} \right)_i^2 V_{\boldsymbol{\theta}_{\boldsymbol{Q}}}(j) \text{Var}\left(\theta_{Q_j}\right) + \sum_{k=1}^{M} \left(\frac{\partial \hat{\mathbf{s}}}{\partial \boldsymbol{\theta}_{\boldsymbol{R}}(k)} \frac{\partial \hat{\mathbf{s}}}{\partial \theta_{R_k}} \right)_i^2 V_{\boldsymbol{\theta}_{\boldsymbol{R}}}(k) \text{Var}\left(\theta_{R_k}\right) \Bigg|_{\boldsymbol{\theta}=\hat{\boldsymbol{\theta}}} \tag{39}$$

Where the subscript i on the right-hand side of ~~equation 39~~ Eq. (39) refers to the i^{th} ~~element~~ entry of the derivative vector which is a scalar and parameters ~~$\boldsymbol{\theta}_{\boldsymbol{Q}}(j)$ and $\boldsymbol{\theta}_{\boldsymbol{R}}(k)$~~ θ_{Q_j} and θ_{R_k} refer to the ~~jth and kth~~ j^{th} and k^{th} parameters of the sets $\boldsymbol{\theta}_{\boldsymbol{Q}}$ and $\boldsymbol{\theta}_{\boldsymbol{R}}$ respectively. From ~~equation 39~~Eq. (39), we can see how uncertainty in the flux estimate is apportioned into variance components of $\boldsymbol{\theta}_{\boldsymbol{Q}}$ and $\boldsymbol{\theta}_{\boldsymbol{R}}$ of an inversion ~~frameworks~~framework. No normalization is necessary in such ~~global sensitivity analysis~~ a framework of GSA since on the right hand side of ~~equation 39~~Eq. (39), the variance components are naturally weighted in such a way that both sides have same units. Once the two components of $V_{\hat{s}_i}$ (i.e. ~~equation 39~~Eq. (39)) are computed, they can also be summed over the solution space (e.g. number of gridcells $\times$ number of time-periods) of $\hat{\mathbf{s}}$ and ranked to find the relative importance of the parameters.

Even after simplification, implementation of ~~equation 39~~ Eq. (39) is difficult as it requires knowledge of the uncertainties associated with the parameters of $\mathbf{Q}$ and $\mathbf{R}$ that are generally not known. Note that, it is also possible to have a complete apportionment of ~~$V_{\hat{\mathbf{s}}}$~~ the variance of $\hat{\mathbf{s}}$ for all the parameters of ~~f (e.g., $\mathbf{Q}, \mathbf{R}, \mathbf{H}, \mathbf{X}(\text{or } \mathbf{s}_{\text{prior}})$, and $\mathbf{z}$)~~ $\mathbf{f}$ at least up to the first-order polynomial in the Taylor's series. However, ~~it's~~ its implementation is difficult since it requires knowledge ~~about~~ of the

covariances of all the parameters. We do not further discuss ~~global sensitivity analysis~~ GSA in the context of the case study presented in this work, but we have shown ~~it's~~ its application with respect to ~~$\mathbf{Q}$ and $\mathbf{R}$~~ $\mathbf{Q}$ and $\mathbf{R}$ in the MATLAB ~~Live script.~~

3.4 ~~Local sensitivity based relative importance of covariates, covariance parameters and observations~~

~~It is easy to compare importance of observations, covariates and covariance parameters within themselves as they have same units. However, the notion of relative importance amongst them is harder for two reasons. First, we need to standardize or normalize the local sensitivities such that they are in same units and preferably bounded (for discussion see Link and Doherty Jr, 2002). All the derivatives in this work result in vectors or matrices that may consist of negative, positive and extreme values and can be in different units. Normalization of parameters with different units has only been applied for scalars (i.e. a single parameter in a simulation model; for details see Saltelli et al., 2008). Normalization of sensitivity matrices is not common in literature. Second, we also need to adopt a technique to compare these senstivity matrices and find their relative importance in influencing .~~ Livescript.

~~One of the ways to address the first problem is via global sensitivity analysis that is described in subsection 3.3. Although, it is a direct approach, it is not tenable in most scenarios. In this work, sensitivity matrices are harmonized via a two-step normalization. For each sensitivity matrix~~ Other than the variance based Taylor series method described above there are many other approaches to perform GSA as described in the introductory section but either they are computationally expensive or assume independence of the input parameters which is not the case in atmospheric inverse problems. We do not pursue other approaches for quantifying GSA associated with $\mathbf{Q}$ and $\mathbf{R}$ as they would lead to similar results and would not add anything substantial to the contributions of this study.

3.4 Ranking importance of covariates, covariance parameters, and observations from LSA

In atmospheric inverse modeling we encounter two situations while ranking importance of parameters. These are ranking of parameters when they have same or different units. The situation of ranking of parameters with same units ~~(like $\frac{\partial \hat{\mathbf{s}}_B}{\partial H_{ij}}$), first, a simple min-max normalization (see Vafaei et al., 2020) is applied to each column to normalize the values between 0 to 1. The normalized columns are then aggregated by groups to form columns representing combined sensitivity of the groups. For example, a group can be observations of a particular instrument or set of estimation points. Then a second step min-max normalization is applied to each of these aggregated columns to transform them to vary between 0 and 1.~~

~~Once the normalized sensitivity vectors are obtained for each quantity of interest, the objective is to compute a score for each of these vectors such that these scores can be ranked.To authors knowledge, no standard methods exist for such comparisons. An approach such as principal component analysis (PCA) (Jolliffe and Cadima, 2016) could have been used to answer this question. However, the underlying question here is to rank the sensitivities with respect to their importance in influencing the estimate of $\hat{\mathbf{s}}$ which cannot be achieved by PCA. Hence, we adopt~~ arise when we want to study the influence of a group of parameters like observations that have same units. Comparatively, the situation of ranking of parameters with different units arise when we want to study the influence of groups of parameters that have different units like observations in $\mathbf{z}$ in

comparison to variance of observations in $\mathbf{R}$. Both these situations can be accounted through GSA that is described in Sec. 3.3. However, GSA in atmospheric inverse modeling cannot be fully performed due to the reasons mentioned earlier. Therefore, in this work we adopted a regression-based approach to ~~assess the relative importance of covariates, covariance parametersand observations. In this work, we~~ rank the importance of parameters. The proposed approach utilizes output from LSA, accounts for multicollinearity and results in importance scores that are bounded between 0 to 1. We define the regression model for ranking as:

$$\mathbf{\Gamma}\hat{\mathbf{s}} = \mathbf{E}\gamma\mathbf{E}\boldsymbol{\gamma} + \xi\boldsymbol{\xi} \tag{40}$$

where ~~$\mathbf{\Gamma}\ \hat{\mathbf{s}}$~~ are fluxes obtained from an inversion, ~~$\mathbf{E}_{(m,\text{number of derivatives})}$ is a~~ and $\mathbf{E}$ is an $(m \times \text{number of derivatives})$ matrix of the previously estimated ~~normalized sensitivitiesor derivatives with dimensions, $\gamma_{(\text{number of derivatives},1)}$ are the unknown coefficients for the sensitivities or derivative vectors, and $\xi_{(m,1)}$ is the unobserved error~~ sensitivities. The vector of unknown coefficients $\boldsymbol{\gamma}$ is of dimension (number of derivatives $\times$ 1), and $\boldsymbol{\xi}$ is an $(m \times 1)$ vector of unobserved errors associated with the regression model. To exemplify, ~~$\mathbf{E}$ in equation 40~~ $\mathbf{E}$ in Eq. (40) can be arranged as:

$$\mathbf{E}\mathbf{E} = \left[\frac{\partial\hat{\mathbf{s}}}{\partial\mathbf{z}}\frac{\partial\hat{\mathbf{s}}}{\partial\mathbf{z}}\ \frac{\partial\hat{\mathbf{s}}}{\partial\mathbf{Q}}\frac{\partial\hat{\mathbf{s}}}{\partial\mathbf{Q}}\ \frac{\partial\hat{\mathbf{s}}}{\partial\mathbf{R}}\frac{\partial\hat{\mathbf{s}}}{\partial\mathbf{R}}\ \cdot\ \cdot\right] \tag{41}$$

~~where γ is the vector of relative importance weights.~~ In a regression-based approach, as described in ~~equation 40~~Eq. (40), multicollinearity between independent variables in ~~$\mathbf{E}$~~ $\mathbf{E}$ can pose a problem for determining the importance of independent variables in influencing ~~$\mathbf{\Gamma}$~~$\mathbf{\Gamma}$. To avoid this problem, we computed relative importance weights by using the method outlined in Johnson, 2000. These weights are computed by first deriving uncorrelated orthogonal counterparts of the ~~independent variables in $\mathbf{E}$~~ covariates in $\mathbf{E}$ and then regressing ~~dependent variable on them $\hat{\mathbf{s}}$~~ to get importance weights for each ~~independent variable~~covariate. The weights are standardized by the coefficient of determination i.e., R^2 such that they range between 0 to 1 with the sum of all the weights being 1. ~~A detailed description~~ Implementation of this method is ~~given in Johnson, 2000 and the implementation of this method is~~ included in the ~~Live script~~ Livescript submitted with this manuscript. ~~Note that an approach of LASSOcould also have been employed here to obtain the relative weights of the predictors~~

Note Least Absolute Shrinkage and Selection Operator (LASSO) or Principal Component Analysis (PCA) can also be employed to compute ranking under multicollinearity. However both these methods result in weights that are unbounded. Furthermore, "inference after selection~~"~~" is ambiguous in linear regression which is the case for LASSO coefficients (see Berk et al., 2013 or chapter 6 of Hastie et al., 2015 for details). Consequently, interpreting the LASSO coefficients as ~~relative importance scores~~ ranks may not be the best approach~~here.Thus, we do not use this technique here.~~.

The regression-based approach described above can be employed when we want to rank parameters with both same and different units. However, an additional normalization step is required if we are interested in getting overall rank of the

parameters that have different units like in $\mathbf{z}$, $\mathbf{Q}$, and $\mathbf{R}$. To perform this normalization, first each column in every sensitivity matrix (e.g. $\frac{\partial \hat{\mathbf{s}}}{\partial \mathbf{z}}$, $\frac{\partial \hat{\mathbf{s}}}{\partial \mathbf{Q}}$, and so forth) that is to be ranked is normalized (min-max normalization; see Vafaei et al., 2020) between 0 to 1. Following which all columns for a sensitivity matrix are summed and renormalized to vary between 0 to 1. This results in one column that is representative of a sensitivity matrix for a particular group. We denote this by the subscript "grouped" (e.g. $\frac{\partial \hat{\mathbf{s}}}{\partial \mathbf{z}_{\text{grouped}}}$) in latter sections.

Once the normalized sensitivity vectors are obtained for each group the regression methodology as described above can be used to rank the importance of each group. The ranking methodology proposed above does not account for non-linear relationship between estimates of the fluxes and the derivatives. If this is a concern then the strength of the nonlinear relationship among the derivative vectors can be first obtained by computing distance correlation between fluxes and the local derivatives of the parameters. After which we can employ variable transformation (e.g., Box-Cox transformation; see Sakia, 1992) before applying the regression methodology described above.

Note that most analytical inversions use DOFS to diagnose information content of an inversion. DOFS = 0 implies that no informational gain happened in an inversion. In this case, the estimated flux reverts back to prior. In ~~Equation 40~~Eq. (40), this means that the ~~γ~~ γ coefficient that corresponds to $\mathbf{Q}$ would ~~be the largest~~ have the largest impact. Likewise if DOFS is large, then ~~γ~~ the γ coefficients for $\mathbf{z}$ and $\mathbf{R}$ ~~should~~ would be larger (and likely correlated). We show this correspondence ~~with standard approaches in section~~in Sec. 4.

Finally, all different kinds of diagnostic methods that are applied in the context of any regression-based model can be used for understanding the relationship between dependent and independent variables. However, what ~~independent variables~~ covariates to include in ~~$\mathbf{E}$~~ $\mathbf{E}$ depends on the specific case study under consideration.

4 Results: Los Angeles methane inversion case study

To demonstrate the applicability of our methods we utilize data from our published work on CH_4 fluxes in the Los Angeles megacity (see Yadav et al., 2019). In this previous work, fluxes were estimated for South Coast Air Basin (SoCAB) region (~~Figure~~see Fig. 3) at 0.03° spatial (1826 grid-cells) and 4-day temporal resolution from the Jan 27, 2015 through Dec 24, 2016. However, in the current work we utilize input data from Oct 23, 2015 through Oct 31, 2015 that is a single inversion period to contextualize the applicability of our methods. This period overlaps with the beginning of the ~~now~~ well-studied Aliso Canyon gas leak (Conley et al., 2016). We do not extend our analysis for the full duration of the previous study as this is not the objective of this work and all the details associated with computing the inverse flux estimates can be found in that work. Furthermore, in the Livescript we present our sensitivity based equations with respect to the geostatistical approach to inverse modeling as this was the approach adopted in the previous study.

For each observation included in the case study, a ~~footprint~~ forward operator was obtained by using Weather Research Forecasting-Stochastic Time Inverted Lagrangian Model (see Yadav et al., 2019). These ~~footprints~~ forward operators are used to demonstrate the application of the methodology for building IOAMI and JSD based correlation matrices in the MATLAB ~~Live script~~Livescript. They are also used in conjunction with measurements, and prior information to estimate the fluxes and perform LSA.

4.1 ~~Spatio-temporal area of dominance (~~STAD ~~)~~ from the ~~footprints~~forward operators

In this work we identify STAD for the 4-day period for which the inversion was performed. The spatial domain of the study over this time period is uniquely disaggregated by STAD as shown in ~~Figure~~Fig. 3. The STAD for different sites are mostly spatially contiguous but for some sites we found isolated grid cells which were not within the contiguous zones. We have manually combined these with STAD for the nearest site to create a spatially continuous map as shown in ~~Figure~~Fig. 3. The discontinuous version of the STAD shown in ~~Figure~~Fig. 3 is included in the Livescript. The discontinuities in the STAD ~~mostly result~~ result mostly from unequal number of observations across sites and indicates that aggregation over longer time-period is required to completely identify a noise free STAD. We do not investigate the time-period of this aggregation as this is beyond the scope of this work.

Overall, the STAD for each site indicates regions of ~~emissions~~ fluxes that contributes most to the observational (e.g. CH4 enhancement) signal. This in turn allows us to sub-divide the spatio-temporal variations in fluxes or enhancements by the ~~STADs~~STAD regions.

4.2 Sensitivity analysis

One of the main goals of the sensitivity analysis after performing ~~inversions~~ an inversion is to identify the observations that had most influence on the flux estimates. ~~Overall assessment of~~ Other than observations it is also important to explore the importance of ~~different~~ other inputs to an inversion~~after observations is also important to explore~~, like variance parameters in **R**. We describe the process of performing this analysis within the context of the case study mentioned in ~~section~~Sec. 4. This section discusses the relative importance of the input quantities in influencing $\hat{s}$ ~~via~~ by utilizing the local sensitivities.

4.2.1 Comparison and ranking of the observations

Importance of the individual measurements in influencing ~~$\hat{s}$~~ $\hat{s}$ can be easily computed through relative importance methodology described in section 3.4. Although, all entries of $\frac{\partial \hat{s}}{\partial \mathbf{z}}$ $\frac{\partial \hat{s}}{\partial \mathbf{z}}$ are in same units, direct ranking of observations or sites without employing relative importance technique can lead to misleading results. This happens due to the presence of large negative and positive values in $\frac{\partial \hat{s}}{\partial \mathbf{z}}$ $\frac{\partial \hat{s}}{\partial \mathbf{z}}$ that are governed by the overall spatio-temporal spread, intensity of ~~footprints, and large observations~~ forward operators, and observations with large enhancements.

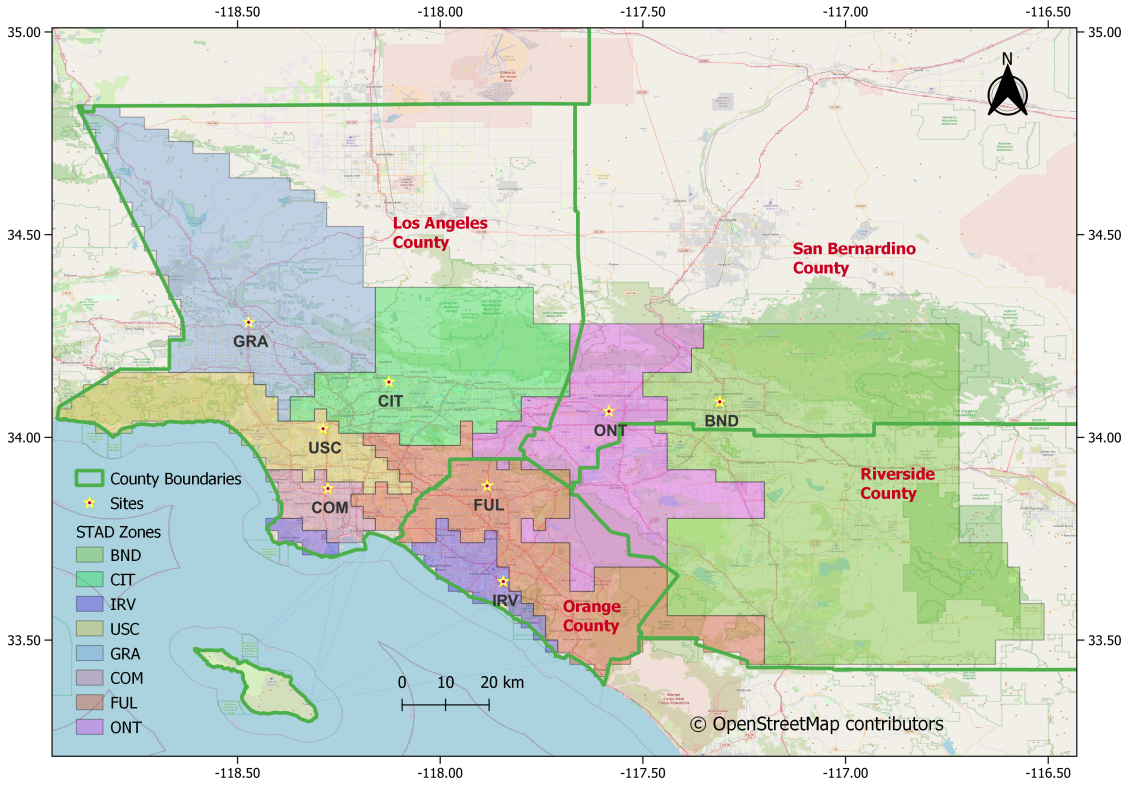

Figure 3. Study area with county boundaries, measurement locations and the Spatio-Temporal Area of Dominance of measurement locations.

Site	Importance Score	Rank
GRA	0.26	1
ONT	0.24	2
COM	0.13	3
IRV	0.11	4
BND	0.10	5
CIT	0.07	6
FUL	0.07	7
USC	0.06	8

Table 1. The importance scores and ranking of 8 sites based on the sensitivity of the estimated fluxes ($\hat{\mathbf{s}}$) to observations ($\mathbf{z}$).

For the case study in this work, we find that observations collected at the GRA site that is located nearest to the source of Aliso Canyon gas leak are most influential in governing $\hat{\mathbf{s}}$ as shown by site-based rankings in Table 1. These rankings primarily

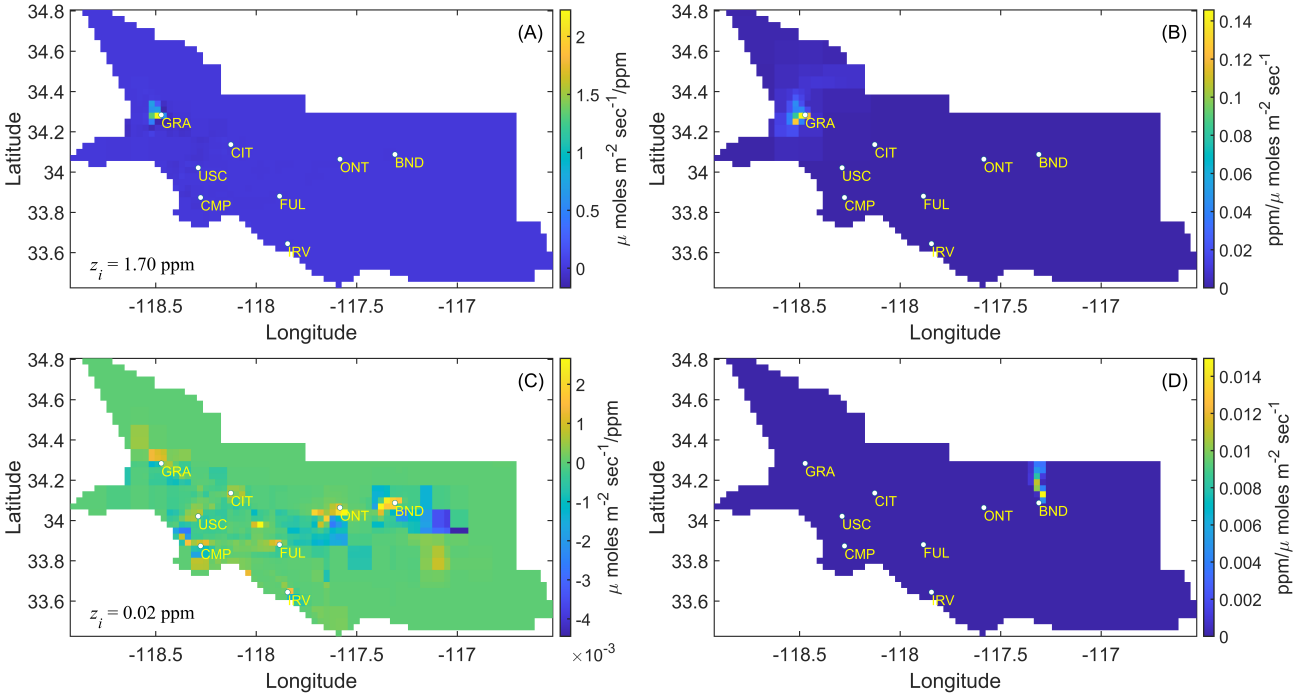

Figure 4. The sensitivities ($\frac{\partial \hat{s}}{\partial \mathbf{z}}$) ~~and footprints ($\mathbf{H}$)~~ ($\frac{\partial \hat{s}}{\partial z_i}$) and forward operator of the most and least important observation in inversions. Subplot A and C show the sensitivity of ~~the estimated fluxes~~ $\hat{s}$ with respect to the most (A) and least important (C) observation. The CH_4 enhancement associated with these observations is shown in the bottom left corner of the subplots and identified by the symbol z_i. The right subplots B and D show ~~footprints~~ forward operators associated with the sensitivities shown in subplots A and C respectively.

show the importance of observations from a site in influencing the estimated fluxes for the time period in consideration. Observation based assessment of $\frac{\partial \hat{s}}{\partial \mathbf{z}}$ $\frac{\partial \hat{s}}{\partial \mathbf{z}}$ resulted in ranking an observation with the largest enhancement of 1.7 ppm to be most important. Contrarily, an observation for the BND site that had an enhancement of 0.02 ppm is found to be least important in influencing ~~$\hat{s}$~~$\hat{s}$. Note this is not an observation with the lowest enhancement but with the lowest influence. The most and least important observation along with their corresponding ~~footprints~~ forward operators are shown in ~~Figure~~Fig. 4.

4.2.2 Relative importance of ~~$\mathbf{Q}, \mathbf{R}, \mathbf{X}, \beta$~~$\mathbf{Q}, \mathbf{R}, \mathbf{X}, \beta$, and ~~$\mathbf{z}$~~$\mathbf{z}$

After the two-step normalization of $\frac{\partial \hat{s}}{\partial \mathbf{z}}, \frac{\partial \hat{s}}{\partial \mathbf{X}}, \frac{\partial \hat{s}}{\partial \mathbf{H}}, \frac{\partial \hat{s}}{\partial \beta}, \frac{\partial \hat{s}}{\partial \mathbf{Q}}$, ~~and~~ $\frac{\partial \hat{s}}{\partial \mathbf{R}}$ $\frac{\partial \hat{s}}{\partial \mathbf{z}}, \frac{\partial \hat{s}}{\partial \mathbf{X}}, \frac{\partial \hat{s}}{\partial \mathbf{H}}, \frac{\partial \hat{s}}{\partial \beta}, \frac{\partial \hat{s}}{\partial \mathbf{Q}}$, and $\frac{\partial \hat{s}}{\partial \mathbf{R}}$ as described in section 3.4, the spatial plots of all these ~~quantities~~ grouped quantities that we call as $\frac{\partial \hat{s}}{\partial \mathbf{z}_{\text{grouped}}}, \frac{\partial \hat{s}}{\partial \mathbf{X}_{\text{grouped}}}, \frac{\partial \hat{s}}{\partial \mathbf{H}_{\text{grouped}}}, \frac{\partial \hat{s}}{\partial \beta_{\text{grouped}}}, \frac{\partial \hat{s}}{\partial \mathbf{Q}_{\text{grouped}}}$, and $\frac{\partial \hat{s}}{\partial \mathbf{R}_{\text{grouped}}}$ can be created to explore the regions of the low and high weights (see Fig. 5) at the grid scale~~as shown in Figure 5~~.

Figure 5 shows that the weights of $\frac{\partial \hat{s}}{\partial \mathbf{X}}$ $\frac{\partial \hat{s}}{\partial \mathbf{X}_{\text{grouped}}}$ is lower in the regions well constrained by the observations. However, ~~the~~ opposite is true in the case of $\frac{\partial \hat{s}}{\partial \mathbf{Q}}$ ~~and~~ $\frac{\partial \hat{s}}{\partial \mathbf{R}}$ $\frac{\partial \hat{s}}{\partial \mathbf{Q}_{\text{grouped}}}$ and $\frac{\partial \hat{s}}{\partial \mathbf{R}_{\text{grouped}}}$. This implies, that data constrained regions have lower

posterior uncertainty thereby increasing the influence of prescribed or estimated uncertainty parameters. There is smoothness in the weights of $\frac{\partial \hat{\mathbf{s}}}{\partial \mathbf{Q}}$ $\frac{\partial \hat{\mathbf{s}}}{\partial \mathbf{Q}_{\text{grouped}}}$ in the domain except around some sites , (ONT, FUL, and IRV), which is an indication that the estimates of $\hat{\mathbf{s}}$ $\hat{\mathbf{s}}$ remain insensitive to the $\mathbf{Q}$ $\mathbf{Q}$ parameter in these regions. These relationships can be quantified by assessing correlation between local sensitivities and $\hat{\mathbf{s}}$ $\hat{\mathbf{s}}$ as shown in FigureFig. 6.

There is strong evidence of multicollinearity among independent variables in explaining the dependent variable covariates in explaining $\hat{\mathbf{s}}$ (e.g. see first column of the figureFig. 6). The direction of the best fit line appears to be in sync with the expectation regarding CH_4 fluxes in the region during that time period. Thus, $\frac{\partial \hat{\mathbf{s}}}{\partial \mathbf{z}}$ $\frac{\partial \hat{\mathbf{s}}}{\partial \mathbf{z}_{\text{grouped}}}$ is positively correlated with $\hat{\mathbf{s}}\hat{\mathbf{s}}$, which implies that higher enhancement in $\mathbf{z}$ $\mathbf{z}$ leads to an increase in the estimated fluxes. Similar to $\frac{\partial \hat{\mathbf{s}}}{\partial \beta}$ Similarly $\frac{\partial \hat{\mathbf{s}}}{\partial \boldsymbol{\beta}_{\text{grouped}}}$ is also positively correlated with $\hat{\mathbf{s}}$ $\hat{\mathbf{s}}$ implying that any increase in the scaling factor increases the estimated fluxes. The negative relationship of $\frac{\partial \hat{\mathbf{s}}}{\partial \mathbf{X}}$ and $\hat{\mathbf{s}}$ $\frac{\partial \hat{\mathbf{s}}}{\partial \mathbf{X}_{\text{grouped}}}$ and $\hat{\mathbf{s}}$ just indicates that an increase in $\frac{\partial \hat{\mathbf{s}}}{\partial \mathbf{X}}$ $\frac{\partial \hat{\mathbf{s}}}{\partial \mathbf{X}_{\text{grouped}}}$ inversely influences the magnitude of the estimated fluxes. This occurs as $\hat{\mathbf{s}}$ $\hat{\mathbf{s}}$ reverts to $\mathbf{X}$ in regions unconstrained by observations whereas opposite happens in areas constrained by observations that in the context of the case study includes sources of largest emissionsfluxes.

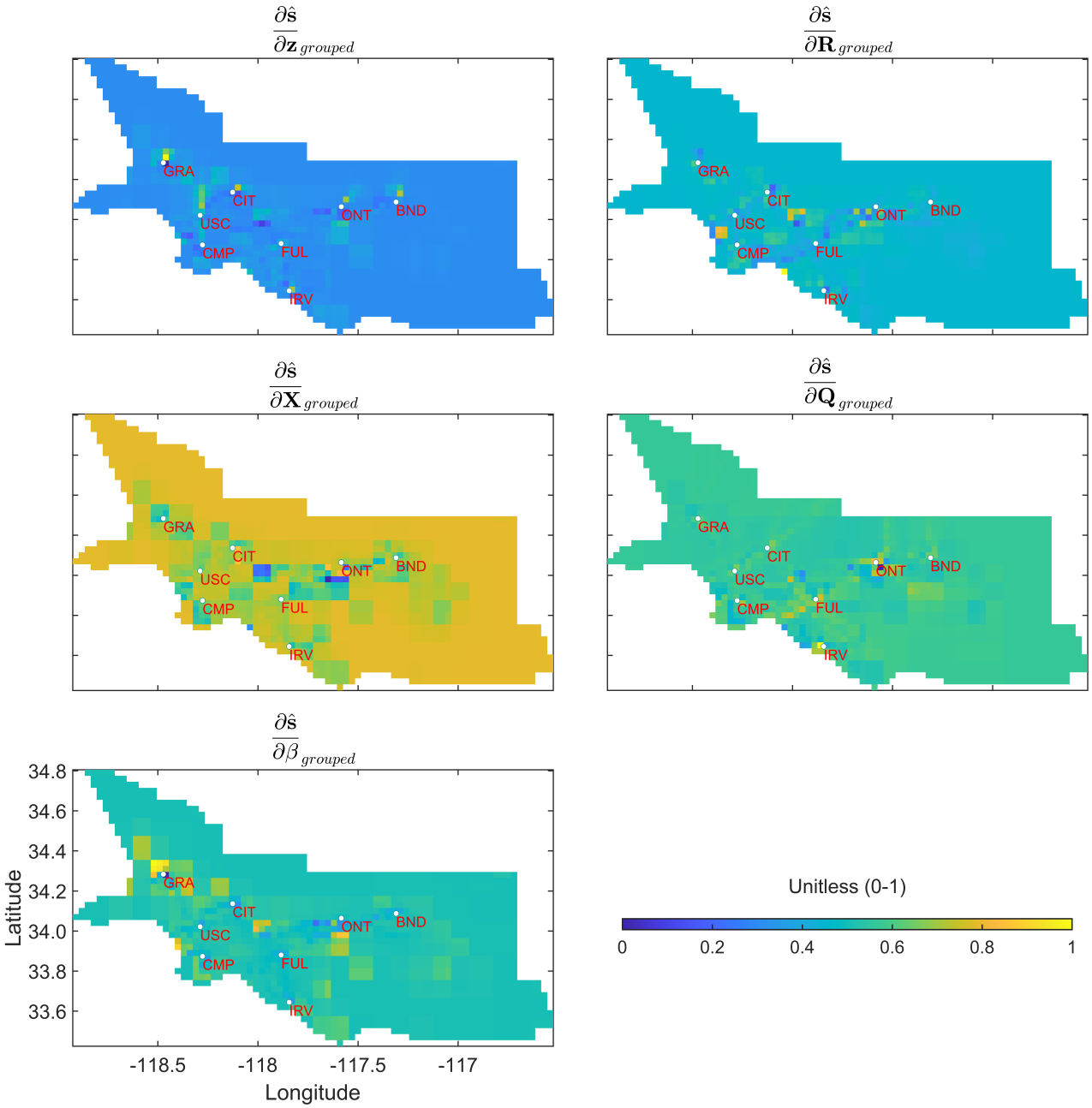

Figure 5. ~~Local~~ Grouped local sensitivities of the estimated fluxes ($\hat{\mathbf{s}}$~~s~~) with respect to $\mathbf{z}$, $\mathbf{R}$, $\mathbf{X}$, $\mathbf{Q}$, and ~~β~~ $\boldsymbol{\beta}$ from top-left to bottom-right respectively. Note, in the case of ~~$\frac{\partial \hat{\mathbf{s}}}{\partial \mathbf{z}}$, $\frac{\partial \hat{\mathbf{s}}}{\partial \mathbf{R}}$, and $\frac{\partial \hat{\mathbf{s}}}{\partial \mathbf{X}}$~~ $\frac{\partial \hat{\mathbf{s}}}{\partial \mathbf{z}_{grouped}}$, $\frac{\partial \hat{\mathbf{s}}}{\partial \mathbf{R}_{grouped}}$, and $\frac{\partial \hat{\mathbf{s}}}{\partial \mathbf{X}_{grouped}}$ two-step normalization is performed to generate subplots associated with these quantities. Derivatives with respect to: (1) observations in $\mathbf{z}$, (2) parameters in $\mathbf{R}$, and (3) entries in $\mathbf{X}$ are normalized between 0 and 1 and then after aggregating these for every grid-cell another Min-Max normalization is performed to limit their ranges between 0 and 1. Only single normalization is performed in case of ~~$\frac{\partial \hat{\mathbf{s}}}{\partial \mathbf{Q}}$ and $\frac{\partial \hat{\mathbf{s}}}{\partial \beta}$~~ $\frac{\partial \hat{\mathbf{s}}}{\partial \mathbf{Q}_{grouped}}$ and $\frac{\partial \hat{\mathbf{s}}}{\partial \boldsymbol{\beta}_{grouped}}$ as they consist of only one parameter.

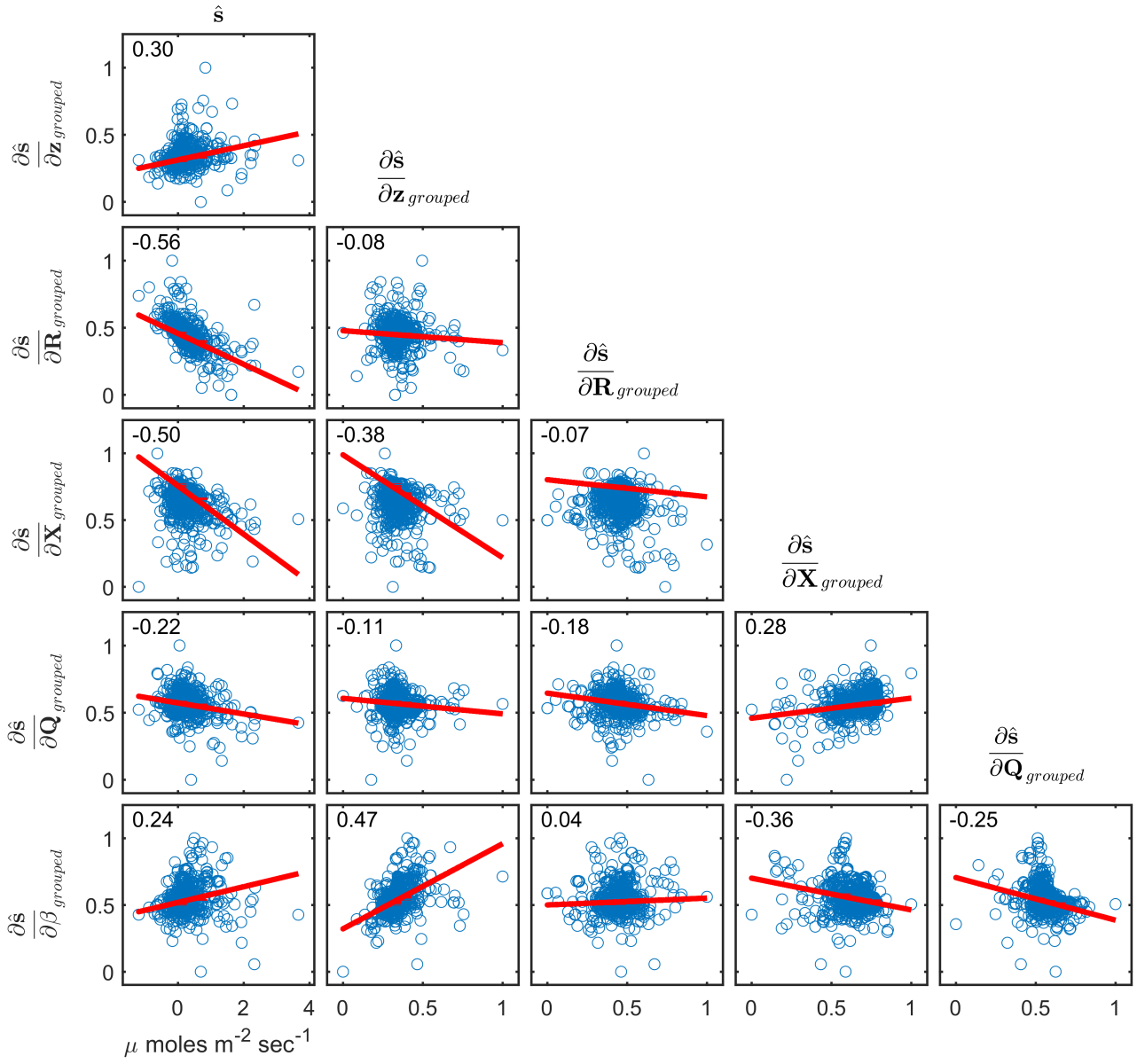

Figure 6. Scatterplots of relationships between ~~ŝ and $\frac{\partial \hat{s}}{\partial \mathbf{z}}$, $\frac{\partial \hat{s}}{\partial \mathbf{R}}$, $\frac{\partial \hat{s}}{\partial \mathbf{X}}$, $\frac{\partial \hat{s}}{\partial \mathbf{Q}}$, $\frac{\partial \hat{s}}{\partial \beta}$~~ ŝ and $\frac{\partial \hat{s}}{\partial \mathbf{z}_{grouped}}$, $\frac{\partial \hat{s}}{\partial \mathbf{R}_{grouped}}$, $\frac{\partial \hat{s}}{\partial \mathbf{X}_{grouped}}$, $\frac{\partial \hat{s}}{\partial \mathbf{Q}_{grouped}}$, $\frac{\partial \hat{s}}{\partial \beta_{grouped}}$. Note as before in ~~Figure~~Fig. 5 all the derivatives are normalized to limit their range between 0 and ~~1 whereas ŝ has units of μmoles^{-1}m^{2}sec^{-1}~~.1. The correlation coefficient of the relationships shown in each scatterplot is reported on the top right corner of the subplots. The least square line of best fit is shown in red color in every subplot.

5 Discussion

This ~~work provides diagnostic tools to investigate components of two inverse modeling framework as well as assesses~~ study lays out techniques to assess the quality of the inferred estimates of fluxes. Sensitivity analysis is an important diagnostic tool to understand the impact of the choices made with respect to inputs on the estimated fluxes. However, it is not a recipe for selecting the proper forms of ~~$\mathbf{X}$ or structure of $\mathbf{Q}$ and $\mathbf{R}$~~ $\mathbf{X}$ or the structure of $\mathbf{Q}$ or $\mathbf{R}$ before performing an inversion. Other tools or methods such as Bayesian Information Criterion, Variance Inflation Factor should be used to perform this task.

The case study in this work is designed only to demonstrate the methodologies described in ~~section~~Sec. 3. We do not impose non-negativity constraints to obtain positive CH_4 fluxes as was done in the original 2019 study (Yadav et al., 2019). This is done because posterior likelihood changes its functional form under non-negativity constraints and the analytical forms of senstivity equations presented in this work become invalid. Thus, some CH_4 fluxes obtained in this study have negative values as can be seen in the map of ~~$\hat{\mathbf{s}}$~~ $\hat{\mathbf{s}}$ in the MATLAB ~~Live script~~Livescript. However, even in these situations assessing sensitivity through an inversion without imposition of non-negativity is useful as it provides insights into the role of $\mathbf{z}$, $\mathbf{R}$, $\mathbf{Q}$, and $\mathbf{X}$ in governing estimates of non-negative $\hat{\mathbf{s}}$.

Like ~~$\mathbf{z}$~~$\mathbf{z}$, the importance of ~~$\mathbf{Q}$ and $\mathbf{R}$~~ $\mathbf{Q}$ and $\mathbf{R}$ parameters can be directly obtained when all parameters have the same units. This happens in the case study presented in this work. However, this is not guaranteed as ~~$\mathbf{R}$~~ $\mathbf{R}$ can be a function of variance parameters and spatio-temporal correlation length expressed in the distance units in space and time. Furthermore, a nonstationary error covariance ~~$\mathbf{R}$~~ $\mathbf{R}$ can have parameters that have even more complicated units. This situation is not limited to ~~$\mathbf{R}$~~ $\mathbf{R}$ and also applies to the prior error covariance ~~$\mathbf{Q}$ and $\mathbf{X}$~~$\mathbf{Q}$ and $\mathbf{X}$. Under these conditions, a comparison between the sensitivity matrices is only possible after normalization. Therefore, for comparative assessment we recommend use of a multiple linear regression based relative importance method to rank these quantities.

The ~~importance of~~ $\frac{\partial \hat{\mathbf{s}}}{\partial \mathbf{z}}$ overall importance of $\frac{\partial \hat{\mathbf{s}}}{\partial \mathbf{z}}$ is best explored by ~~first~~ performing column based normalization and then employing the relative importance method. Additionally, column based normalization can be augmented by row-based normalization to assess and rank the influence of observations in governing gridscale estimates of ~~$\hat{\mathbf{s}}$~~$\hat{\mathbf{s}}$. Qualitatively, column and row-based assessment increase our understanding about the spatio-temporal estimates of ~~$\hat{\mathbf{s}}$~~$\hat{\mathbf{s}}$. This is especially important when point sources are the dominant sources of emissions. Moreover, it also provides an insight into temporal aggregation error (e.g. Thompson et al., 2011) as the information encoded in an instantaneous measurement can get lost over the coarser time-period of inversion. This aggregation error also manifests spatially and is determined by the resolution at which fluxes are obtained. Note in many situations these aggregation errors are unavoidable as the choice of the spatio-temporal resolution of inversions is governed by the density of observations in space and time.

Other than aggregation error, the aggregation of the estimated fluxes also has profound implications as it affects the robustness of the estimated fluxes. It can be proved (see Appendix A) that aggregation of ~~$\hat{s}$~~ $\hat{s}$ in space and time from an inversion conducted at finer resolution leads to reduction in uncertainty. However, even though ratio of observations to the estimated fluxes increases the number of fluxes uniquely resolved declines at coarser resolution (see Appendix B).

~~Computing~~ The computational cost to calculate analytical partial derivatives is minimal as it is a onetime operation and is bounded by the computational cost to perform matrix multiplications, which at max is $O(n^3)$. For the case study presented in this work we can compute analytical derivatives and rank approximately 4000 parameters in few minutes on a laptop. Computing derivatives by using the Kronecker form of ~~the local sensitivities (equations 20, 23 through 26, and 35 though 38~~equations (Eq. (20), (23) through (26), and (35) though (38)) is faster for small problems. However for large inverse problems the storage costs associated with these equations can become prohibitive. In these situations, we propose the use of ~~ij~~ ij form of the equations (~~equations 22, 27 through 30, and 31 though 34~~Eq. (22), (27) through (30), and (31) though (34)) for assessment. Furthermore, computational problems can also arise in ~~importance ranking~~ ranking the inputs if we have large number derivatives (e.g. greater than 10,000) as ~~relative importance method uses~~ the ranking method used in this work relies on eigen value decomposition that has $O(n^3)$ computational complexity. To overcome this problem we advise grouping of derivatives to reduce the dimension of the problem.

Finally, the estimation of STAD and the importance of sites can be influenced by data gaps therefore is not advised in presence of vast differences in the number of observations between sites. ~~Furthermore, if observations from different platforms (e.g. aircraft, satellites and in-situ sites) are used in an inversion then combined ranking of observational platforms is untenable as spatio-temporal densities of measurements are different across platforms.~~

6 Conclusions

Our work makes novel and major contributions that can significantly improve understanding of linear atmospheric inverse problems. It provides: (1) a ~~way to understand the correlations in the footprints or atmospheric transport model, and (2) a~~ framework for post hoc analysis of the impact of inputs on the estimated fluxes and (2) a way to understand the correlations in the forward operators or atmospheric transport model. The authors are not aware of any work where local sensitivities with different units are compared to rank the importance of inputs ~~to an inversion~~ in a linear atmospheric inverse model.

With respect to ~~footprints~~forward operators, we provide mathematical foundations for IOAMI, and Jensen-Shannon based metrics. These two metrics can be used to construct and accommodate a non-stationary error covariance for atmospheric transport component of the model-data mismatch matrix ~~R~~**R**. Furthermore, IOAMI based assessments can be extended to identify STAD from ~~footprints that~~ forward operators that can help in disaggregating regions of influence of the observations over a chosen temporal duration. This assists in understanding the connection between the sources of ~~emissions~~ fluxes and observa-

tions from a particular measurement location.

The IOAMI and JSD based metrics provide an important insight into the two critical and only required components for an inversion that is observations and ~~footprints~~ forward operators (e.g., influence of an observation to ~~sources of emissions~~ the sources of fluxes through STAD). This task can be accomplished prior to conducting an inversion and should be complimented by post hoc LSA, which is a necessity for understanding the behavior of an inverse model. Overall, LSA can answer questions like for which locations and in what order of precedence was an observation important in influencing the estimated fluxes. This kind of analysis is entirely different from estimating uncertainty that tells us reduction in the prior uncertainty due to observations.

LSA is not a replacement for statistical tests that check the underlying assumptions and model specifications ~~of~~ in inverse models. Neither is it a recipe for selecting inputs to an inverse model. However, it has an important role as explained above that can lead to an improved understanding of an atmospheric inverse model.

Code and data availability. All the code and data utilized in this study are submitted as supplementary material.

Appendix

Here we show the proofs of two mathematical statements on the robustness and quality of the estimated fluxes as mentioned in ~~section~~Sec. 5. First, we show why marginal variance of the estimated fluxes (which is the diagonal of covariance matrix of ~~$\hat{s}$~~$\hat{\mathbf{s}}$) decrease when estimated fluxes are post aggregated to a coarser scale or upscaled (A). Second, we show why in such case the model resolution (also termed as, total information resolved by the observations) also decreases (B). Note that, the nomenclature used in the appendix should not be confused with the nomenclature introduced in ~~section~~Sec. 3. The abbreviations and symbols used here are independent of what are used in the ~~section~~Sec. 3.

Appendix A: Proof of the reduction of marginal variance of ~~$\hat{s}$~~ $\hat{\mathbf{s}}$ when upscaling is performed

Post inversion upscaling of any flux field ~~s~~ $\mathbf{s}$ is equivalent to ~~premultiplication~~ pre-multiplication by a weight matrix (in fact, a row stochastic matrix). This can be written as:

$$\tilde{\mathbf{s}} = \mathbf{J}\hat{\mathbf{s}} \tag{A1}$$

Where ~~$\mathbf{J}$~~ $\mathbf{J}$ is a row stochastic (i.e. row-sums are all unity) ~~$k \times p$~~ $k \times m$ weight matrix (~~$k < p$~~$k < m$). Variance of ~~$\tilde{\mathbf{s}}$~~ $\tilde{\mathbf{s}}$ can be written as ~~$\mathbf{J\Sigma J^t}$~~ $\mathbf{J\Sigma J}^t$ where var($\tilde{\mathbf{s}}\tilde{\mathbf{s}}$) = ~~$\mathbf{J}$var($\hat{\mathbf{s}}$)$\mathbf{J^t}$~~ $\mathbf{J}$var($\hat{\mathbf{s}}$)J^t=~~$\mathbf{J\Sigma J^t}$~~ $\mathbf{J\Sigma J}^t$. The general structure of ~~$\mathbf{J}$~~ $\mathbf{J}$ is as follows:

$$J = \begin{bmatrix} 0 & j_{12} & j_{13} & \mathbf{0} & \mathbf{0} & \mathbf{0} \\ j_{21} & \mathbf{0} & j_{2r+1} & j_{2r+2} & \mathbf{0} & \mathbf{0} \\ \vdots & \vdots & \ddots & \ddots & \vdots & \vdots \\ \mathbf{0} & \mathbf{0} & \mathbf{0} & j_{km} & \mathbf{0} & \mathbf{0} \end{bmatrix} = \begin{bmatrix} \mathbf{j}_1^t \\ \mathbf{j}_2^t \\ \vdots \\ \mathbf{j}_k^t \end{bmatrix} \tag{A2}$$

~~Essentially, $\mathbf{J}$~~ However, $\mathbf{J}$ is mostly sparse and values in few places. Rest of the entries are zeros. Essentially, $\mathbf{J}$ can have any number of non-zero entries in a row that may or may not be consecutive. This is because although on a map, adjacent grids are averaged, they may not be adjacent upon vectorization. Moreover, geometry of the map may not be exactly square or rectangular. This means, depending on the upscaling factor and geometry, for any particular grid, there may or may not any neighboring grid for averaging. However, the rows are linearly independent as nearby grids are considered once for averaging.

~~Zeros are represented as dots in the example structure of $\mathbf{J}$ (A2). So, the properties of $\mathbf{J}$~~ The properties of $\mathbf{J}$ are as follows:

1. ~~$\mathbf{J1} = \mathbf{1}$ or $\sum_{j=i}^{p} j_{ij} = 1 \ \forall i = 1, \ldots, k$~~ $\mathbf{J1} = 1$ or $\mathbf{j}_i^t \mathbf{1} = 1 \quad \forall i = 1, 2, \cdot, \cdot, k$
2. ~~$\mathbf{j}_i' \mathbf{j}_l = \mathbf{0}$ for $i \neq l$~~ $\mathbf{j}_i^t \mathbf{j}_k = 0$ for $i \neq r$

We can rearrange the columns of ~~$\mathbf{J}$~~ $\mathbf{J}$ and the rows of ~~$\mathbf{\Sigma}$~~ $\mathbf{\Sigma}$ accordingly without loss of any structure such that non-zero ~~elements~~ entries are consecutive for each row of ~~$\mathbf{J}$. Matrix $\mathbf{J\Sigma J'}$~~ $\mathbf{J}$. Matrix $\mathbf{J\Sigma J'}$ under column permutation can be written as:

$$\mathbf{J\Sigma J^t} = \mathbf{J}_{\pi}\mathbf{\Sigma}_{\pi}\mathbf{J}_{\pi}^t = \underbrace{\begin{bmatrix} \mathbf{l}_1^t & 0 & \ldots & 0 \\ 0 & \mathbf{l}_2^t & \ldots & 0 \\ \vdots & \vdots & \ddots & . \\ 0 & 0 & \ldots & \mathbf{l}_k^t \end{bmatrix}}_{k \times pk \times m} \underbrace{\begin{bmatrix} \mathbf{\Xi}_{11} & \mathbf{\Xi}_{12} & \ldots & \mathbf{\Xi}_{1k} \\ \mathbf{\Xi}_{21} & \mathbf{\Xi}_{22} & \ldots & . \\ \vdots & \vdots & \ddots & . \\ \mathbf{\Xi}_{k1} & . & \ldots & \mathbf{\Xi}_{kk} \end{bmatrix}}_{p \times pm \times m} \overbrace{\begin{bmatrix} \mathbf{l}_1 & 0 & \ldots & 0 \\ 0 & \mathbf{l}_2 & \ldots & 0 \\ \vdots & \vdots & \ddots & . \\ 0 & 0 & \ldots & \mathbf{l}_k \end{bmatrix}}^{p \times k} \tag{A3}$$

$$= \overbrace{\begin{bmatrix} \mathbf{l}_1^t \mathbf{\Xi}_{11} \mathbf{l}_1 & . & \ldots & \mathbf{l}_1^t \mathbf{\Xi}_{1k} \mathbf{l}_k \\ . & \mathbf{l}_2^t \mathbf{\Xi}_{22} \mathbf{l}_2 & \ldots & . \\ \vdots & \vdots & \ddots & . \\ \mathbf{l}_k^t \mathbf{\Xi}_{k1} \mathbf{l}_1 & . & \ldots & \mathbf{l}_k^t \mathbf{\Xi}_{kk} \mathbf{l}_k \end{bmatrix}}^{k \times k} \tag{A4}$$

where ~~$\mathbf{J}^p$ and Σ^p are the column and row permuted $\mathbf{J}$~~ $\mathbf{J}_{\pi}$ and $\mathbf{\Sigma}_{\pi}$ are the permuted $\mathbf{J}$ and Σ respectively. However, for notational clarity, we use $\mathbf{l}$ and $\mathbf{\Xi}$ as the sub-vector and sub-block-matrix of the $\mathbf{J}_{\pi}$ and $\mathbf{\Sigma}_{\pi}$ respectively. Note that, any ~~$\mathbf{J}_i^{p\prime}$~~ $\mathbf{l}_i^t$ is a row-vector of dimension $(1, d_i)$, and ~~Σ_{ii}^p~~ $\mathbf{\Xi}_{ii}$ is a square matrix of dimension (d_i, d_i) where ~~$\sum_{i=1}^{k} d_i = p$~~ $\sum_{i=1}^{k} d_i = m$. Thus, diagonal entry ~~$\mathbf{J}_i^{p\,t} \mathbf{\Sigma}_{ii}^p \mathbf{J}_i^p$~~ $\mathbf{l}_i^t \mathbf{\Xi}_{ii} \mathbf{l}_i$ is a scalar quantity. For any i^{th} diagonal entry, the corresponding scalar quantity can be written as ~~$\sum_{jl} a_{ij}^p a_{il}^p \sigma_{jl}^p$ where superscript p refers to the corresponding matrix after permutation~~ $\sum_{jrl} l_{ij} l_{ir} \Xi_{jr}$. By symmetry of ~~$\mathbf{\Sigma}^p$~~$\mathbf{\Xi}$, this reduces to

$$\mathbf{l}_i^t \boldsymbol{\Xi}_{ii} \mathbf{l}_i = \sum_l a_{il}^p l_{ir}{}^2 \sigma_{ll}^p \Xi_{lr}{}^2 + 2 \sum_{j>l} a_{j>r} l_{ij}{}^p a_{ij}^p \sigma_{jl}^p l_{ir} \Xi_{jr} \tag{A5}$$

By Cauchy Squartz inequality on ~~$\sigma_{jl}^p \Xi_{jr}$~~, this can be written as

$$\sum_l a_{il}^p l_{ir}{}^2 \sigma_{ll}^p{}^2 - 2 \sum_{j>l} a_{j>r} l_{ij}{}^p a_{ij}^p l_{ir} \sigma_{jj}{}^p \sigma_{llrr}^p \leq \sum_l a_{il}^p l_{ir}{}^2 \sigma_{llrr}^p{}^2 + 2 \sum_{j>l} a_{j>r} l_{ij}{}^p a_{il} l_{ij}{}^p \sigma_{jljr}^p \leq \sum_l a_{il}^p l_{ir}{}^2 \sigma_{llrr}^p{}^2 + 2 \sum_{j>l} \tag{A6}$$

$$\left(a_{i1}^p \sqrt{\sigma_{i1}^p} l_{ir} \sqrt{\sigma_{ir}} - \sum_{l \geq 2} a_{il}^p \sqrt{\sigma_{il}^p} r_{\geq 2} l_{ir} \sqrt{\sigma_{ir}} \right)^2 \leq \sum_l a_{il}^p l_{ir}{}^2 \sigma_{llrr}^p{}^2 + 2 \sum_{j>l} a_{j>r} l_{ij}{}^p a_{il} l_{ij}{}^p \sigma_{jj}{}^p \sigma_{llrr}^p \leq \left(\sum_{il} a_{il}^p \sqrt{\sigma_{ll}^p} i_r l_{ir} \sqrt{\sigma_{rr}} \right. \tag{A7}$$

$$\min_l r \sigma_{llrr}^p \left(a_{i1}^p l_{ir} - \sum_{l \geq 2} a_{il}^p r_{\geq 2} l_{ir} \right)^2 \leq \sum_l a_{il}^p l_{ir}{}^2 \sigma_{llrr}^p{}^2 + 2 \sum_{j>l} a_{j>r} l_{ij}{}^p a_{il} l_{ij}{}^p \sigma_{jj}{}^p \sigma_{llrr}^p \leq \max_l r \sigma_{llrr}^p \left(\sum_{il} a_{il}^p i_r l_{ir} \right. \tag{A8}$$

This implies (by property 1 of the weight matrix ~~JJ~~) that the ~~ith diagonal element~~ i^{th} diagonal entry is bounded by:

$$\min_l r \sigma_{llrr}^p \left(a_{i1}^p l_{ir} - \sum_{l \geq 2} a_{il}^p r_{\geq 2} l_{ir} \right)^2 \leq \mathbf{J}_\mathbf{i}' \boldsymbol{\Sigma}_{\mathbf{ii}} \mathbf{J}_\mathbf{i} \leq \max_l r \sigma_{llrr}^p \leq \sum_{r=1}^{d_i} \sigma^p{}_{rr} \tag{A9}$$

where ~~$\sum_{r=1}^{d_i} \sigma^p{}_{rr}$~~ $\sum_{r=1}^{d_i} \sigma_{rr}$ is the sum of the marginal variance of the ith block of un-averaged ~~$\hat{\mathbf{s}}$~~$\hat{\mathbf{s}}$. Thus, sum of the marginal variance of ~~$\tilde{\mathbf{s}}$~~ $\tilde{\mathbf{s}}$ which is the sum of the ~~ith diagonal $\mathbf{J}\mathbf{p}_\mathbf{i}{}^\mathbf{t} \boldsymbol{\Sigma}_{\mathbf{ii}} \mathbf{J}\mathbf{p}_\mathbf{i}$~~ i^{th} diagonal $\mathbf{J}_i^t \boldsymbol{\Sigma}_{ii} \mathbf{J}_i$ is also smaller or equals to the sum total of marginal variance of ~~$\hat{\mathbf{s}}$~~$\hat{\mathbf{s}}$. Clearly, we see that under upscaling or averaging, diagonal of the variance matrix shrinks in magnitude from the un-averaged one. As a consequence, it implies that marginal variance of the posterior mean decreases.

Appendix B: Proof of the reduction in model resolution when upscaling is performed

Upscaled ~~footprint operator $\tilde{\mathbf{H}}$~~ forward operator $\tilde{\mathbf{H}}$ can be written as:

$$\tilde{\mathbf{H}} = HB\mathbf{HB} \quad \text{where } \mathbf{B} \text{ is the upscaling matrix} \tag{B1}$$

Dimension ~~$\mathbf{B}$ is~~ of $\mathbf{B}$ has the dimension of transpose of ~~J. Form of $\mathbf{B}$~~ $\mathbf{J}$. Structual form of $\mathbf{B}$ is similar to ~~form of $\mathbf{J}$~~ the form of $\mathbf{J}$ explained in A2. Non-zero entries of ~~$\mathbf{B}$~~ $\mathbf{B}$ are in the same place as ~~$\mathbf{J}'$ with magnitude being~~ $\mathbf{J}'$ with magnitude replaced by unity. This is evident from the fact that ~~footprint~~ forward operator is summed instead of ~~average over the same grids~~ being averaged for upscaling. Properties of ~~$\mathbf{B}$~~ $\mathbf{B}$ are as follows:

1. ~~$\mathbf{B1} = \mathbf{1}$~~ $\mathbf{B1} = \mathbf{1}$

2. ~~$\mathbf{JB} = \mathbf{diag}(\mathbf{N})^{\mathbf{k}\times\mathbf{k}}$~~ $\mathbf{JB} = diag(\mathbf{N})^{k\times k}$ where ~~$\mathbf{N}$~~ $\mathbf{N}$ is the vector of number of neighboring ~~grids~~ gridcells for any particular ~~grid~~ ~~$\mathbf{N}$~~ $\mathbf{N} = (N_1, \ldots, N_k)$

3. ~~$\mathbf{BJ} = \begin{bmatrix} \mathbf{C_1} & \mathbf{0} & \ldots & \mathbf{0} \\ \mathbf{0} & \mathbf{C_2} & \ldots & \mathbf{0} \\ \vdots & \vdots & \ddots & . \\ \mathbf{0} & . & \ldots & \mathbf{C_k} \end{bmatrix}^{\mathbf{p}\times\mathbf{p}}$~~ $\mathbf{BJ} = \begin{bmatrix} \mathbf{C_1} & \mathbf{0} & \ldots & \mathbf{0} \\ \mathbf{0} & \mathbf{C_2} & \ldots & \mathbf{0} \\ \vdots & \vdots & \ddots & . \\ \mathbf{0} & . & \ldots & \mathbf{C_k} \end{bmatrix}^{m\times m}$ is a block diagonal matrix. Any block ~~$\mathbf{C_i}$ of $\mathbf{JA}$~~ $\mathbf{C}_i$ of $\mathbf{JA}$ can be expressed as a varying dimension (depending on the number of neighboring grids of any particular ~~grid~~gridcell) matrix of form:

$$\mathbf{C}_i = \begin{bmatrix} \frac{1}{N_i} & \cdots & \frac{1}{N_i} \\ \vdots & \ddots & \vdots \\ \frac{1}{N_i} & \cdots & \frac{1}{N_i} \end{bmatrix}^{N_i \times N_i} = \frac{1}{N_i}' \mathbf{1}\mathbf{1}^t \tag{B2}$$

4. ~~$\mathbf{BJ}$~~ $\mathbf{BJ}$ is symmetric and positive semi-definite

~~Proof: $Det(\mathbf{BJ} - \lambda\mathbf{I}) = \mathbf{Det}(\mathbf{C_1} - \lambda\mathbf{I}) \ldots \mathbf{Det}(\mathbf{C_k} - \lambda\mathbf{I})$~~First three properties are simple observations from the construction. So, here we provide proof of the fourth property.

Proof. By construction, $Det(\mathbf{BJ} - \lambda\mathbf{I}) = Det(\mathbf{C_1} - \lambda\mathbf{I}) \ldots Det(\mathbf{C_k} - \lambda\mathbf{I})$. So, eigen values of ~~$\mathbf{BJ}$~~ $\mathbf{BJ}$ are the list of eigen values of the block matrices. It can be proved that 1 and 0 are the only two distinct eigen values of ~~$\mathbf{C_i}$~~ $\mathbf{C}_i$ for any i. Below here is a brief argument on that:

~~$\left(\frac{1}{N_i}\mathbf{1}\mathbf{1}'\right)\mathbf{1}\left(\frac{1}{N_i}\mathbf{1}\mathbf{1}^t\right)\mathbf{1} = \frac{1}{N_i}\mathbf{1}\mathbf{N_i} = \mathbf{1}\cdot\mathbf{1}\ \frac{1}{N_i}\mathbf{1}N_i = \mathbf{1}\cdot\mathbf{1}$~~ implies one eigen value of ~~$\mathbf{C_i}$~~ $\mathbf{C_i}$ is 1. Observe that, ~~$rank\left(\frac{1}{N_i}\mathbf{1}\mathbf{1}'\right) = rank(\mathbf{1}) =$~~ Hence, dimension of null space ~~$dim\left(\mathcal{N}\left(\frac{1}{N_i}\mathbf{1}\mathbf{1}'\right)\right) = k - rank\left(\frac{1}{N_i}\mathbf{1}\mathbf{1}'\right) = k - 1$~~ $dim\left(\mathcal{N}\left(\frac{1}{N_i}\mathbf{1}\mathbf{1}^t\right)\right) = k - rank\left(\frac{1}{N_i}\mathbf{1}\mathbf{1}^t\right) = k - 1$. This implies that the other eigen value of ~~$\mathbf{C_i}$~~ $\mathbf{C_i}$ is 0 with multiplicity $k - 1$.

So, not only ~~$\mathbf{C_i}$~~ $\mathbf{C}_i$ is symmetric but also the eigen values ~~$\mathbf{C_i}$~~ $\mathbf{C}_i$ are always non negative. Consequently, all eigen values of ~~$\mathbf{BJ}$~~ $\mathbf{BJ}$ are of similar form ~~or $\mathbf{BJ}$~~ i.e. $\mathbf{BJ}$ is symmetric positive semidefinite. □

~~Model~~ Finally, model resolution matrix for inversion can be written as ~~$\frac{\partial\hat{\mathbf{s}}}{\partial\mathbf{z}}\mathbf{H}$ where $\mathbf{H}$ is the footprint operator~~ $\frac{\partial\hat{\mathbf{s}}}{\partial\mathbf{z}}\mathbf{H}$ where $\mathbf{H}$ is the forward operator operator. Post inversion aggregated model-resolution can be written as:

$$\frac{\partial\tilde{\mathbf{s}}}{\partial\mathbf{z}}\tilde{\mathbf{H}} = \mathbf{A}\frac{\partial\hat{\mathbf{s}}}{\partial\mathbf{z}}\mathbf{H}\mathbf{B} \quad \text{By equation A1 and B1}\text{By Eq. (A1) and B1} \tag{B3}$$

The question is what happens to the trace of the model-resolution under the upscaled case? We ~~prove it~~ provide a proof for the simple batch Bayesian case in lemma B. Proof for the geostatistical case is similar and left for the enthusiastic readers.

Lemma 1.

$$\mathbf{Mres} = \mathbf{QH'}\boldsymbol{\psi}^{-1}\mathbf{H}$$

$$\mathbf{Mres}_{aggregated} = \mathbf{JQH'}\boldsymbol{\psi}^{-1}\mathbf{HB} \quad \textit{by B3, then then}$$

$$trace() trace\left(\mathbf{Mres}_{aggregated}\right) \leq trace(\mathbf{Mres}) \tag{B4}$$

~~Proof:~~

Proof. Model resolution for the aggregated case can be written as:

$$trace() trace\left(\mathbf{Mres}_{aggregated}\right) = trace trace(\mathbf{JQH'}\boldsymbol{\psi}^{-1}\mathbf{HB}) = trace trace(\mathbf{BJQH'}\boldsymbol{\psi}^{-1}\mathbf{H}) = trace trace(\mathbf{WS}) \text{ where } \mathbf{W} = \mathbf{BJ}, \mathbf{S} = \tag{B5}$$

Where ~~S and W~~ S and W are both of dimension ~~$p \times p$. S~~ $(m \times m)$. S is a positive semidefinite matrix since both ~~Q and $\mathbf{H'}\boldsymbol{\psi}^{-1}\mathbf{H}$~~ Q and $\mathbf{H'}\boldsymbol{\psi}^{-1}\mathbf{H}$ are positive semidefinite. For ~~$\mathbf{W}^{p\times p}$ and $\mathbf{S}^{p\times p}$~~ $\mathbf{W}^{m\times m}$ and $\mathbf{S}^{m\times m}$ positive semidefinite, trace of their product can be bounded by the following quantities (see Kleinman and Athans, 1968 and discussion in Fang et al., 1994):

$$\lambda_{min}(\mathbf{W})trace(\mathbf{S}) \leq trace(\mathbf{WS}) \leq \lambda_{min}(\mathbf{W})trace(\mathbf{S}) \tag{B6}$$

By Property 4 of the weight matrix ~~B~~B, we know that ~~$\lambda_{min}(\mathbf{W}) = 0$ and $\lambda_{max}(\mathbf{W}) = 1$~~ $\lambda_{min}(\mathbf{W}) = 0$ and $\lambda_{max}(\mathbf{W}) = 1$, hence the above reduces to ~~$0 \leq trace(\mathbf{WS}) \leq 1 \cdot trace(\mathbf{S})$~~ $0 \leq trace(\mathbf{WS}) \leq 1 \cdot trace(\mathbf{S})$. Hence is the proof by B5.

□

Author contributions. V.Y., and S.G. contributed equally in preparing the manuscript.

Competing interests. The authors declare no competing interest.

Acknowledgements. The authors thank Anna Karion, Kimberly Mueller, James Whetstone (National Institute of Standards and technology, NIST), and Daniel Cusworth (University of Arizona, UA) for their review and advice on the manuscript. This work was partially funded by NIST's Greenhouse Gas Measurements Program. Support to University of Notre Dame provided by NIST grant 70NANB19H132. Support for JPL was provided via an interagency agreement between NIST and NASA. A portion of this research was carried out at JPL, California Institute of Technology, under a contract with NASA (80NM0018D0004).

References

Berk, R., Brown, L., Buja, A., Zhang, K., and Zhao, L.: Valid post-selection inference, The Annals of Statistics, pp. 802–837, 2013.

Bouchard, M., Jousselme, A.-L., and Doré, P.-E.: A proof for the positive definiteness of the Jaccard index matrix, International Journal of Approximate Reasoning, 54, 615–626, 2013.

Brasseur, G. P. and Jacob, D. J.: Modeling of atmospheric chemistry, Cambridge University Press, 2017.

Cha, S.-H.: Comprehensive survey on distance/similarity measures between probability density functions, City, 1, 1, 2007.

Conley, S., Franco, G., Faloona, I., Blake, D. R., Peischl, J., and Ryerson, T.: Methane emissions from the 2015 Aliso Canyon blowout in Los Angeles, CA, Science, 351, 1317–1320, 2016.

Constantine, P. G. and Diaz, P.: Global sensitivity metrics from active subspaces, Reliability Engineering & System Safety, 162, 1–13, 2017.

Enting, I. G.: Inverse problems in atmospheric constituent transport, Cambridge University Press, 2002.

Fang, Y., Loparo, K. A., and Feng, X.: Inequalities for the trace of matrix product, IEEE Transactions on Automatic Control, 39, 2489–2490, 1994.

Gelman, A. and Hill, J.: Data analysis using regression and multilevel/hierarchical models, Cambridge university press, 2006.

Ghosh, S., Mueller, K., Prasad, K., and Whetstone, J.: Accounting for transport error in inversions: An urban synthetic data experiment, Earth and Space Science, 8, e2020EA001 272, 2021.

Gourdji, S., Hirsch, A., Mueller, K., Yadav, V., Andrews, A., and Michalak, A.: Regional-scale geostatistical inverse modeling of North American CO 2 fluxes: a synthetic data study, Atmospheric Chemistry and Physics, 10, 6151–6167, 2010.

Groen, E. A., Bokkers, E. A., Heijungs, R., and de Boer, I. J.: Methods for global sensitivity analysis in life cycle assessment, The International Journal of Life Cycle Assessment, 22, 1125–1137, 2017.

Gurney, K. R., Law, R. M., Denning, A. S., Rayner, P. J., Baker, D., Bousquet, P., Bruhwiler, L., Chen, Y.-H., Ciais, P., Fan, S., et al.: TransCom 3 CO2 inversion intercomparison: 1. Annual mean control results and sensitivity to transport and prior flux information, Tellus B: Chemical and Physical Meteorology, 55, 555–579, 2003.

Hamby, D. M.: A review of techniques for parameter sensitivity analysis of environmental models, Environmental monitoring and assessment, 32, 135–154, 1994.

Hastie, T., Tibshirani, R., and Wainwright, M.: Statistical learning with sparsity, Monographs on statistics and applied probability, 143, 143, 2015.

Heijungs, R.: Identification of key issues for further investigation in improving the reliability of life-cycle assessments, Journal of Cleaner Production, 4, 159–166, 1996.

Johnson, J. W.: A heuristic method for estimating the relative weight of predictor variables in multiple regression, Multivariate behavioral research, 35, 1–19, 2000.

Jolliffe, I. T. and Cadima, J.: Principal component analysis: a review and recent developments, Philosophical Transactions of the Royal Society A: Mathematical, Physical and Engineering Sciences, 374, 20150 202, 2016.

Kitanidis, P. K.: On the geostatistical approach to the inverse problem, Advances in Water Resources, 19, 333–342, 1996.

Kleinman, D. and Athans, M.: The design of suboptimal linear time-varying systems, IEEE Transactions on Automatic Control, 13, 150–159, 1968.

Lauvaux, T., Miles, N. L., Deng, A., Richardson, S. J., Cambaliza, M. O., Davis, K. J., Gaudet, B., Gurney, K. R., Huang, J., O'Keefe, D., et al.: High-resolution atmospheric inversion of urban CO2 emissions during the dormant season of the Indianapolis Flux Experiment (INFLUX), Journal of Geophysical Research: Atmospheres, 121, 5213–5236, 2016.

Lin, J., Gerbig, C., Wofsy, S., Andrews, A., Daube, B., Davis, K., and Grainger, C.: A near-field tool for simulating the upstream influence of atmospheric observations: The Stochastic Time-Inverted Lagrangian Transport (STILT) model, Journal of Geophysical Research: Atmospheres, 108, 2003.

Link, W. A. and Doherty Jr, P. F.: Scaling in sensitivity analysis, Ecology, 83, 3299–3305, 2002.

MacKay, D. J., Mac Kay, D. J., et al.: Information theory, inference and learning algorithms, Cambridge university press, 2003.

MatlabLivescript: version 9.9.0 (R2020b), The MathWorks Inc., Natick, Massachusetts, https://www.mathworks.com/help/matlab/matlab_prog/what-is-a-live-script-or-function.html.

Michalak, A. M., Bruhwiler, L., and Tans, P. P.: A geostatistical approach to surface flux estimation of atmospheric trace gases, Journal of Geophysical Research: Atmospheres, 109, 2004.

Michalak, A. M., Randazzo, N. A., and Chevallier, F.: Diagnostic methods for atmospheric inversions of long-lived greenhouse gases, Atmospheric Chemistry and Physics, 17, 7405–7421, 2017.

Morris, M. D.: Factorial sampling plans for preliminary computational experiments, Technometrics, 33, 161–174, 1991.

Nielsen, F.: On the Jensen–Shannon symmetrization of distances relying on abstract means, Entropy, 21, 485, 2019.

Rabitz, H.: Systems analysis at the molecular scale, Science, 246, 221–226, 1989.

Rödenbeck, C., Houweling, S., Gloor, M., and Heimann, M.: Time-dependent atmospheric CO2 inversions based on interannually varying tracer transport, Tellus B: Chemical and Physical Meteorology, 55, 488–497, 2003.

Rödenbeck, C., Conway, T., and Langenfelds, R.: The effect of systematic measurement errors on atmospheric CO 2 inversions: a quantitative assessment, Atmospheric Chemistry and Physics, 6, 149–161, 2006.

Rodgers, C. D.: Inverse methods for atmospheric sounding: theory and practice, vol. 2, World scientific, 2000.

Sakia, R. M.: The Box-Cox transformation technique: a review, Journal of the Royal Statistical Society: Series D (The Statistician), 41, 169–178, 1992.

Saltelli, A., Ratto, M., Andres, T., Campolongo, F., Cariboni, J., Gatelli, D., Saisana, M., and Tarantola, S.: Global sensitivity analysis: the primer, John Wiley & Sons, 2008.

Sobol, I. and Kucherenko, S.: Derivative based global sensitivity measures, Procedia-Social and Behavioral Sciences, 2, 7745–7746, 2010.

Sobol, I. M.: Global sensitivity indices for nonlinear mathematical models and their Monte Carlo estimates, Mathematics and computers in simulation, 55, 271–280, 2001.

Sudret, B.: Global sensitivity analysis using polynomial chaos expansions, Reliability engineering & system safety, 93, 964–979, 2008.

Tarantola, A.: Inverse problem theory and methods for model parameter estimation, SIAM, 2005.

Thompson, R., Gerbig, C., and Rödenbeck, C.: A Bayesian inversion estimate of N 2 O emissions for western and central Europe and the assessment of aggregation errors, Atmospheric Chemistry and Physics, 11, 3443–3458, 2011.

Turányi, T.: Sensitivity analysis of complex kinetic systems. Tools and applications, Journal of mathematical chemistry, 5, 203–248, 1990.

Vafaei, N., Ribeiro, R. A., and Camarinha-Matos, L. M.: Selecting normalization techniques for the analytical hierarchy process, in: Doctoral Conference on Computing, Electrical and Industrial Systems, pp. 43–52, Springer, 2020.

Wikle, C. K. and Berliner, L. M.: A Bayesian tutorial for data assimilation, Physica D: Nonlinear Phenomena, 230, 1–16, 2007.

Xu, C. and Gertner, G.: Understanding and comparisons of different sampling approaches for the Fourier Amplitudes Sensitivity Test (FAST), Computational statistics & data analysis, 55, 184–198, 2011.

Yadav, V., Duren, R., Mueller, K., Verhulst, K. R., Nehrkorn, T., Kim, J., Weiss, R. F., Keeling, R., Sander, S., Fischer, M. L., et al.: Spatio-temporally resolved methane fluxes from the Los Angeles Megacity, Journal of Geophysical Research: Atmospheres, 124, 5131–5148, 2019.